

P-West High Intensity Secondary Beam Area

Design Report March, 1977

B. Cox
Project Physicist

**R. Currier, D. Eartly, A. Guthke, G. Johnson,
D. Lee, R. Oram, E. Villegas**
Mechanical Design

J. Rest, E. Tilles, P. Vander Arend
Cryogenic and LCW Design

S. Orr, A. Visser
Electrical Design

**E. Major, T. Pawlak, J. Raczek,
G. Valdez, M. Warner**
Architectural Services

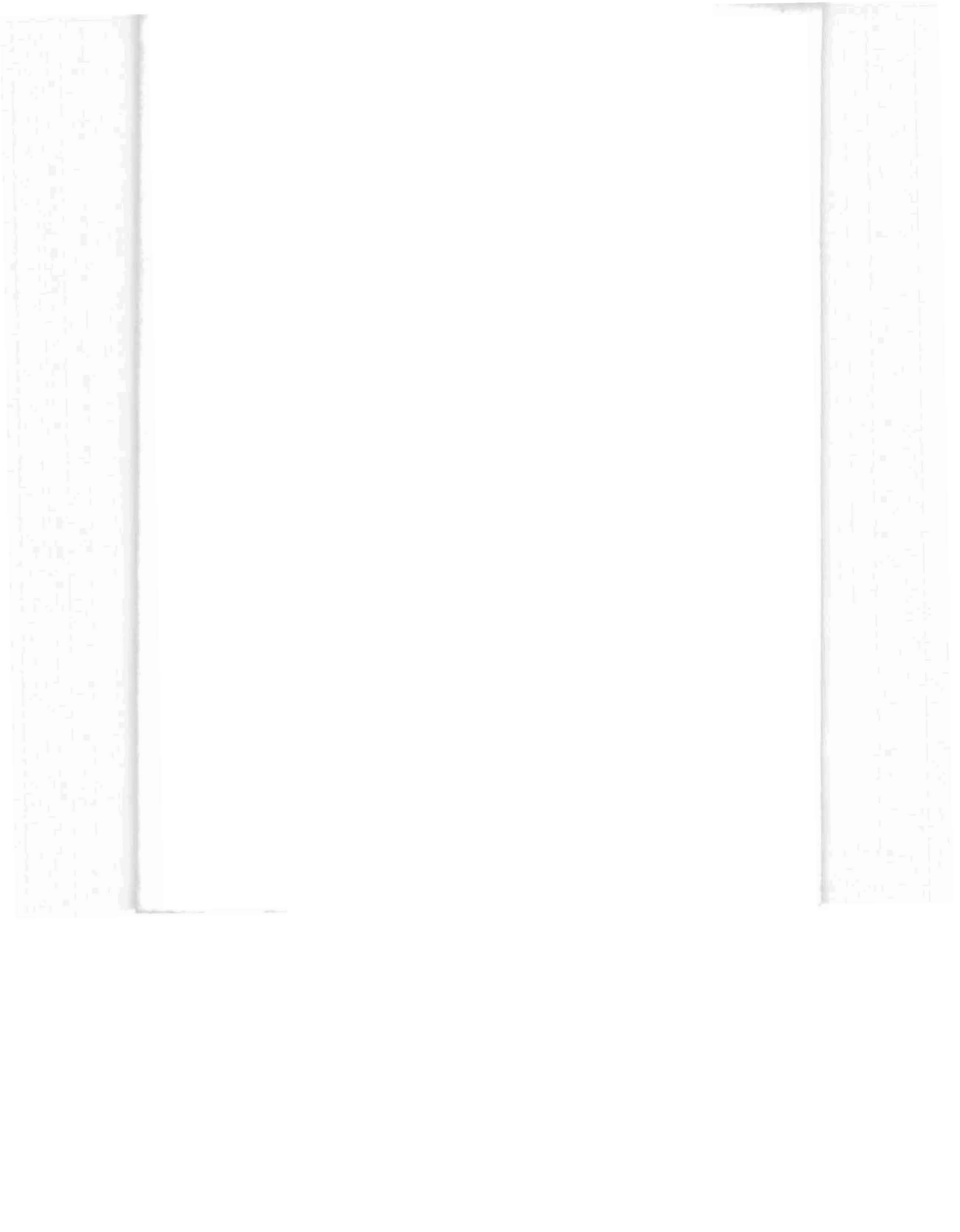
C. Rotolo
Instrumentation

R. Scherr, R. Sorber
Radiation Safety

Fermi National Accelerator Laboratory
Batavia, Illinois



Operated by Universities Research Association, Inc., under contract with
the United States Energy Research and Development Administration



SUMMARY

This report gives the initial design parameters of a 1000 GeV High Intensity Superconducting Secondary Beam Laboratory to be situated in the Proton Area downstream of the existing Proton West experimental station. The area will provide Fermilab with a major capability for experimentation with pion and antiproton beams of intensities and of energies available at no other laboratory and with an electron beam with excellent spot size, intensity, and purity at energies far above that available at electron machines. Detailed beam design, area layouts, and cost estimates are presented, along with the design considerations.



TABLE OF CONTENTS

I. General Description

	Page
A. Proton Beam Transport (Downstream Area of P-West)	1
B. Proton Beam Targeting Area	2
C. High Intensity Superconducting Secondary Beam Channel	3
D. Experimental Area	4

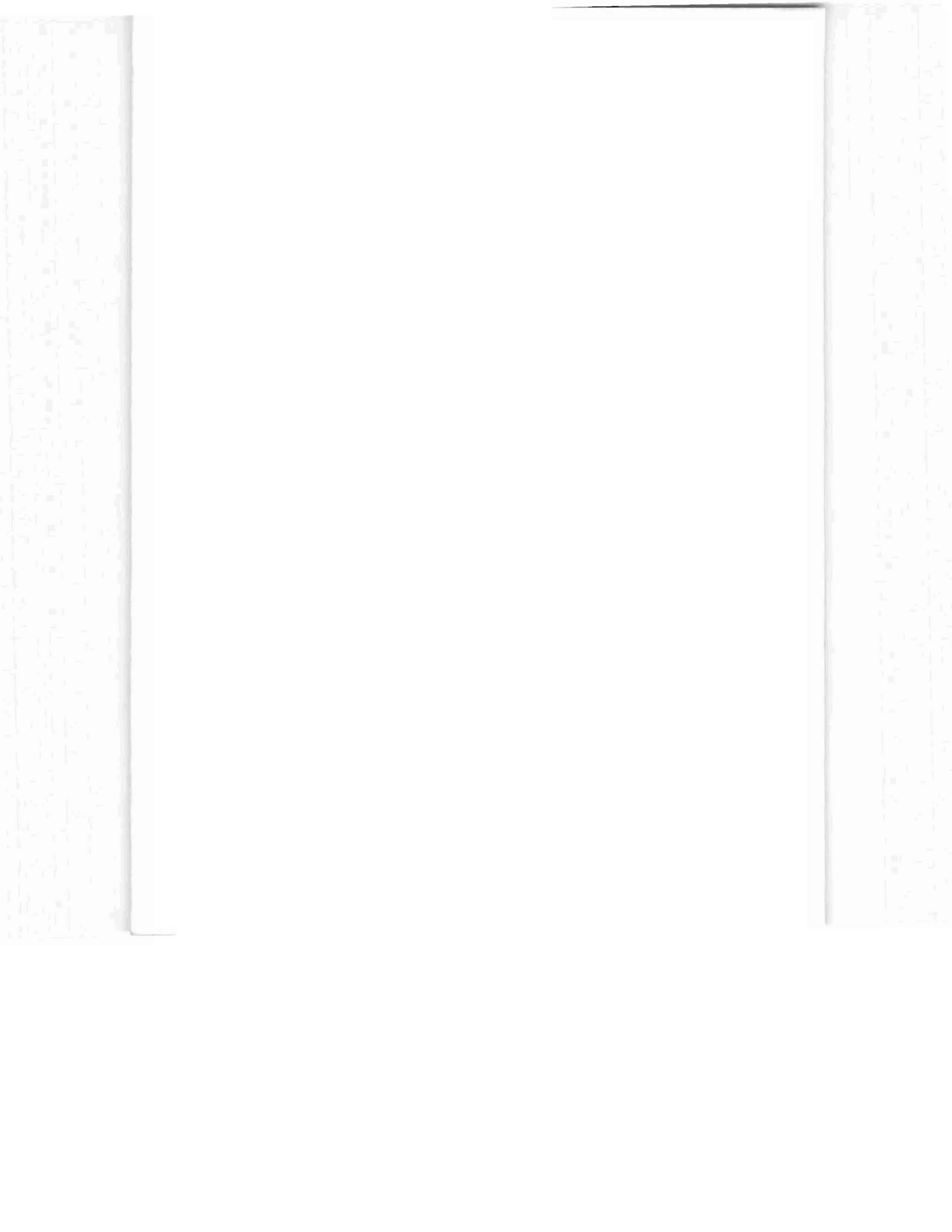
II. Technical Appendices

A. Radiation Safety	7
1. Shielding Calculations	7
2. Interlock System	9
B. High Intensity Pion Beam Cryogenic System	11
a. Introduction	11
b. Summary	11
c. Refrigeration Load of the System	12
d. Transfer Line (2400 Amp Design)	12
e. Transfer Line (200 Amp Design)	13
f. Satellite Refrigerator	14
g. Cryogenic Design of the Magnet	14
C. Electrical Design	15
a. The DC System	15
The Quenching Circuit	16
b. DC Distribution System	17
Power Distribution and Loads	17
Secondary Distribution	17
Motor Control Center	18
D. Mechanical Design	19
1. Target Box Design	19
2. Beam Dump	20
3. Momentum Slit	22

	Page
4. Transporter Design 22
5. LCW System 23
E. Instrumentation 27
Beam Line Instrumentation. 27
Cryogenic Instrumentation 29
<u>III. Acknowledgments</u>	
Acknowledgments 31

LIST OF TABLES

	Page
Table Ia. Superconducting Transport (To F1)	32
Table Ib. Conventional 300-GeV Transport System.	33
Table II. High Intensity Laboratory Minimum Magnet Specifications.	34
Table III. High Intensity Transport Focal Properties (Focused and Parallel Beam)	35
Table IV. Pion Beam - Estimated Power Requirements	36
Table V. Instrumentation Requirements	37
Table VI. Schedule	38
Table VIIa. Plant Cost Estimate Summary	39
Table VIIb. Equipment Estimate (1000 GeV Configuration)	40



LIST OF FIGURES

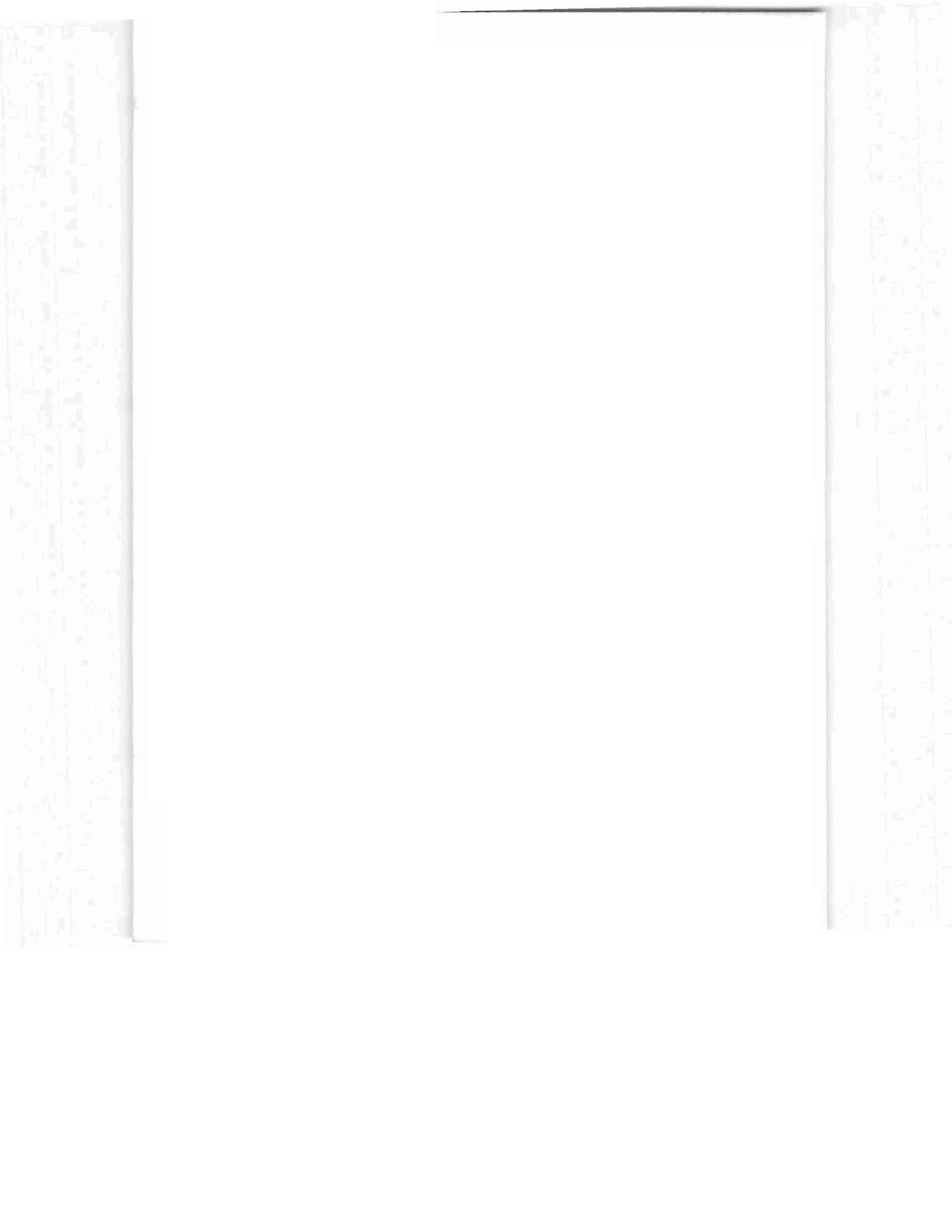
	Page
Fig. 1. High Intensity Beam Area - Plan View - Magnet Layout - Beam Optics	42
Fig. 2(a). Proton Targeting Station (PW-3)	43
Fig. 2(b). Proton Beam Targeting Configurations	44
Fig. 2(c). Energy Deposition Curves - Proton Beam Dump	45
Fig. 3(a). Secondary Beam Spot Size (rms half-width) vs. Proton Target Spot Size (FWHM)	46
Fig. 3(b). Secondary Beam Spot vs. Angular Acceptance (F4)	47
Fig. 3(c). Secondary Beam Spot Size vs. Momentum Bite (F4)	48
Fig. 3(d). Secondary Beam Parallelism vs. Momentum Bite (F4)	49
Fig. 3(e). Secondary Beam Parallelism vs. Angular Acceptance (F4)	50
Fig. 4. Experimental Area and Service Building (PW-5)	51
Fig. 5(a). π^{\pm} Yields vs. Angular Acceptance 400 GeV	52
Fig. 5(b). π^{\pm} Yields vs. Momentum Bite (Wang Fits)	53
Fig. 5(c). π^{\pm} Yields vs. Energy of the Secondary Beam	54
Fig. 5(d). π^{\pm} Yields vs. Energy of the Proton Beam	55
Fig. 6(a). Radiation Levels in PW-3 During Operation of PW-1 Area	56
Fig. 6(b). "Minimal" Triangular Steel Shield Configuration	57
Fig. 7. 3000 Amp Transfer Line and Conductor	58
Fig. 8. 3000 Amp Transfer Box	59
Fig. 9. Helium Circuit Drawing at Magnet.	60
Fig. 10. 200 Amp Transfer Line	61
Fig. 11. Inter-Magnet Helium Plumbing	62
Fig. 12. Superconducting Magnet Power Supply with Built In Quenching Circuit	63
Fig. 13. Electrical Power Flow Diagram	64
Fig. 14. Target Box	65
Fig. 15. Be Target Assembly	66

	Page
Fig. 16. Beam Dump67
Fig. 17. Momentum Slit68
Fig. 18. Transporter69
Fig 19. Pion Lab Cooling Water System.70

1. General Description [REDACTED]

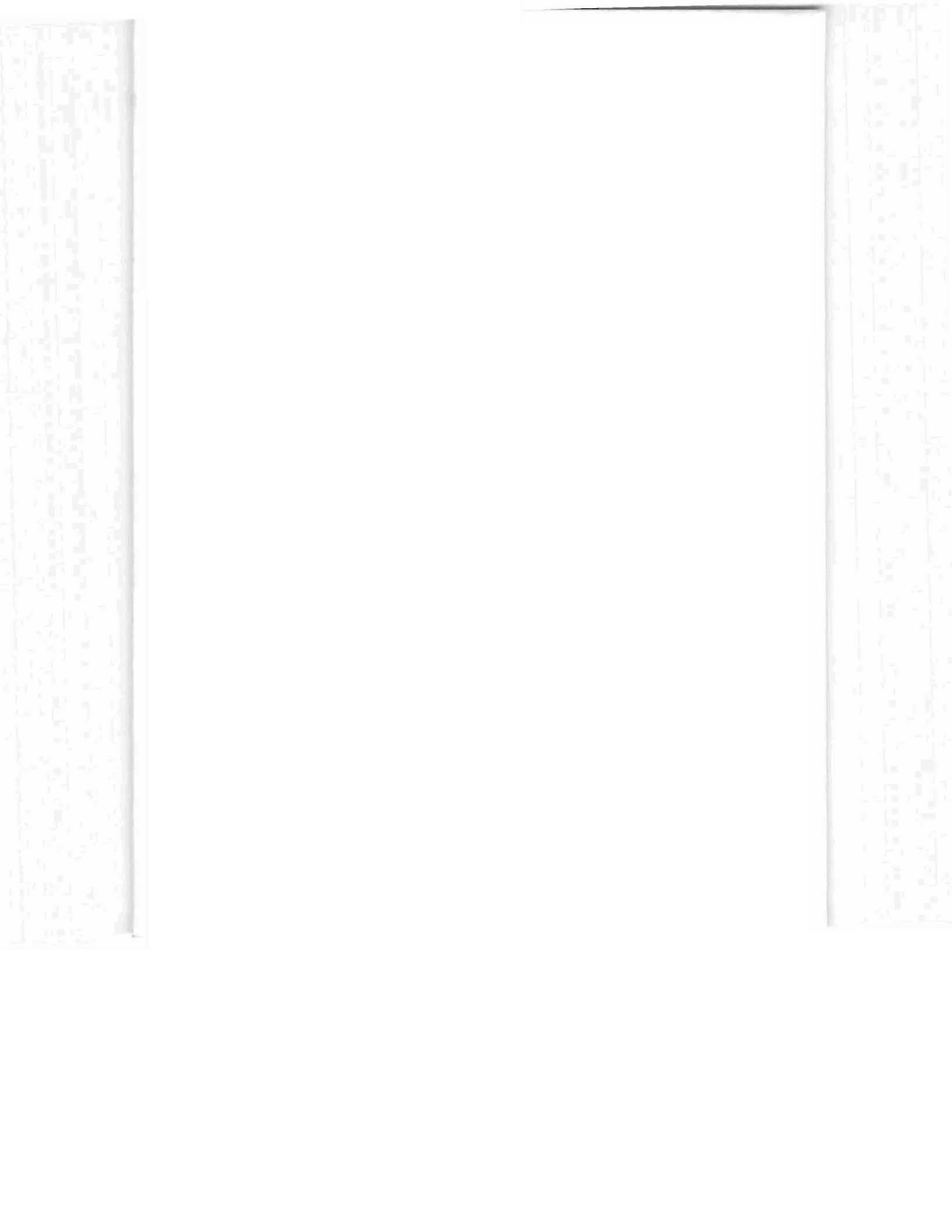
2. Technical Appendices [REDACTED]

3. Acknowledgments [REDACTED]



General Description [REDACTED]

[REDACTED]



P-WEST HIGH INTENSITY SECONDARY BEAM AREA

DESIGN REPORT

I. GENERAL DESCRIPTION

In response to the growing experimental interest in low cross section effects in which large beam intensities are needed, a secondary beam area has been designed which would provide Fermilab with a zero degree secondary charged beam of an intensity far surpassing that available elsewhere. The magnitude and the scope of this area is set by the following basic goals:

1. This area must be capable of targeting 1000 GeV protons and fluxes of 10^{14} protons/pulse at 500 GeV.
2. The secondary beam should have the maximum intensity π possible and be tunable from 100 GeV/c to 1000 GeV/c with either positive or negative flux. This transport should be capable of producing a high quality electron beam and an enriched antiproton beam. In addition, it should be capable of transporting the proton beam to the experimental hall.
3. This beam should be a high quality (i.e., small spot size or high parallelism) beam in both planes.
4. A transmission target station should be maintained in PW1 and the construction and operation of the secondary beam area should interfere as little as possible with the execution of the P-West proton beam physics program.

The combination of high energy and high intensity desired in this area immediately implies that the most economical and feasible plan is one in which superconducting elements are used in all possible places. The layout of Figure 1 and Column 3 of Table Ia gives the final 1000 GeV/c configuration of the high intensity beam, assuming use of superconducting quadrupoles and dipoles currently being developed at Fermilab, and assumes the development of sextupoles of suitable strengths.

Columns 1 and 2 of this same table show the configurations of the intermediate stages of installation of 500 GeV proton targeting with a 400 GeV secondary beam and 1000 GeV targeting with an 800 GeV secondary beam. In addition, in Table Ib, the alternative of a 300 GeV conventional beam is presented along with power estimates for the operation of such a beam.

A. PROTON BEAM TRANSPORT (Downstream Area of P-West)

The configuration of the superconducting area, as shown in Figure 1, starts with a refocussing of the primary proton beam in the

downstream end of the existing P-West enclosure, onto a target 130' downstream of the current P-West dump. A possible targeting configuration of the proton beam with the PW1 experimental area in use gives spot sizes and divergences (FWHM):

$$\theta_x = .21 \text{ mrad}$$

$$X = .21 \text{ cm}$$

$$\theta_y = .56 \text{ mrad}$$

$$Y = .03 \text{ cm}$$

at the target point for the secondary beam using the measured emittance of the extracted proton beam ($\epsilon_H = .44 \pi$, $\epsilon_V = .16 \pi$ mm-mrad). After refocussing, the proton beam is deflected horizontally to the west by three superconducting dipoles by 10.97 mrad through a channel in the P-West proton dump and a 100' length of 6" pipe onto the production target of the secondary beam. When accesses are made to the secondary beam targeting enclosure, the current is automatically reversed in this safety bend and protons deflected 10.97 mrad to the East and dumped at the end of P-West. This reversed deflection ensures that the intense muon cone that arises in the dump is maximally deflected away from the production target enclosure (PW-3). Furthermore, this targeting enclosure is protected by a 105' triangular steel shield immediately upstream of it. Thus, it would be possible with this system to continue to run proton experiments in P-West when work is being done in PW-3. The calculation of the shielding effect of this system is presented in Appendix D1. The services for both this area and the targeting area PW-3, discussed below, are housed in Service Building P3, shown in Figure 1 to the west of PW-3.

B. PROTON BEAM TARGETING AREA

The factors that enter into the design of the target box area PW-3 are:

1. The production angle of the charged secondary beam must be varied from 0° to 7.315 mrad in order to enhance the \bar{p}/π^- ratio.
2. Both positive and negative beams must be possible.
3. The capability of generating a zero degree neutral beam from the target must be maintained.
4. There must be as much momentum dispersion inside the target shielding as possible in order to momentum-select the flux entering the initial superconducting quadrupole triplet in the secondary beam transport. This is necessary since it is not possible to transport the lower energy flux below the tune point of the secondary beam cleanly through the flux gathering triplet to the momentum slit (Enclosure

PW-4). Without this momentum dispersion, the flux defocused into the superconducting conductor may exceed the nominal limit of 10^7 minimum ionizing/cm³, and difficulties may be encountered in keeping the magnets from going normal at these radiation levels. Estimates of the level of radiation after the collimator-dump system in PW-3 have been made and are discussed in Appendix D.1.

In order to accomplish these objectives, the targeting arrangement of Figures 2a and 2b has been designed. The proton beam entering PW-3 from P-West is bent horizontally to the west by two superconducting 10' dipoles by angles ranging from 0° to 7.315 mrad. The horizontal displacement of the beam at the target caused by this deflection is compensated by a dogleg, the first half of which is in the existing Proton West, and the second half of which is at the upstream end of PW-3. The targeting system itself consists of a one interaction length water-cooled Be target, followed by a water-cooled conical aperture collimator embedded in a 5' thick steel wall. This device makes the initial flux definition of the secondary beam (see Appendix D). Following this collimator, a main ring B-2 magnet selects the sign of, disperses and deflects the flux from the target into the secondary beam channel, defined by a 20' variable aperture⁶ collimator. The momentum dispersion inherent in this system is adequate to sweep out all charged particles below .6 p, where p is the tune point of the beam. The conical aperture is set by inserts to match the transverse momentum accepted by the geometry of the secondary beam transport. We have considered apertures of .75, 1.25, and 1.85 mrad, half-angle. See Figure 5a.

C. HIGH INTENSITY SUPERCONDUCTING SECONDARY BEAM CHANNEL

The high intensity beam area extending from PW-3 to PW-5 (experimental hall) contains a superconducting secondary channel capable of transporting and containing a 10% momentum bite of either 0° positive or negative flux to a target placed at F1. This point is a simultaneous X, Y dispersion-free focus with the Y (vertical) plane sextupole corrected. This transport is tunable between 100 and 1000 GeV/c. A summary of the properties of the beam is given in Table III. The chromatic sextupole aberrations inherent in such a beam are minimized in the non-dispersive Y plane by the coupled sextupoles placed at the X foci of the beam. The first order structure of the beam is chosen to minimize the X chromatic aberrations. The beam is composed basically of sets of quadrupole triplets for reasons of their symmetric acceptance and magnifications, and because the aberrations induced with this beam structure are much less than with the comparable doublet structure. The spot size vs. momentum bite curves for this beam are shown in Figure 3.

While the geometric acceptance of the first quadrupole triplet is 300 μ steradian %, the actual beam channel acceptance is defined by the collimator inside the 50' target box area, and the blowup of the beam inside the quadrupoles in the FODO part of the beam.

Therefore the final beam acceptance is 18 μ steradian % with sextupoles on and 60 μ steradian % with sextupoles off. As mentioned in the previous section, the first part of the channel after the target contains a 20', 22 kg B2 magnet, which provides a dispersion capable of sweeping low momentum tracks out of the 0° channel when the beam is tuned to higher momentum (i.e., the flux below 470 GeV/c if the beam is tuned to 750 GeV/c). This dispersion precludes the difficulty of trying to transport all of the charged particle flux of both signs through the first flux gathering superconducting triplet.

The first quadrupole triplet, as shown in Figure 1, takes the flux passing out of the target box through the angular aperture of the dump and, in combination with the dipoles immediately downstream of the triplet, forms a horizontal (X plane) dispersed Y focus at the momentum slit and a dispersed X focus further downstream at the position of the first sextupole correction elements. At the momentum slit, we expect a dispersion of 2.94 mm/% and an X spot of 3.4 mm for $\frac{\Delta p}{p} = \pm .5\%$ and, therefore, no

difficulty in varying the momentum bite accepted in this beam from 1% to 10%. At the dispersed X focus are placed the first sextupole correction elements which form the first half of a sextupole doublet. Between this sextupole set and the equal strength coupled sextupole set further downstream, there is a set of three bends and eight quadrupoles set to alternating polarities to form a FODO channel. The purpose of this structure is to form a non-dispersive X focus at which the conjugate sextupole set is placed, and to produce a transfer matrix (R) between these sextupoles which is identically - I. When the sextupoles are energized, the geometric aberrations that they produce cancel, and the chromatic aberrations in the Y plane can be corrected without the usual attendant degradation of the Y spot at F1 or F2 due to induced geometric aberrations. The X spot is unaffected by the sextupoles since they are placed at X focii.

The final section of the transport consists of a targeting triplet which produces focii at F1, F2, and F3 in the experimental area. See Figure 4 and Table III for the positions and properties of each of these focii. The yield curves for π^{\pm} for the F1 focii are shown in Figures 5a - 5d. For F4, the downstream-most focal point, this triplet produces a parallel beam which passes through a 150' \bar{p} tagging Cerenkov and is refocussed onto the F4 target by an additional set of targeting quadrupoles in the experimental area. The properties of this parallel beam are also given in Table III. More detailed discussion of the \bar{p} and e^{-} options are contained in other reports now in preparation.

D. EXPERIMENTAL AREA

The plan view of the experimental area and its relationship to the experimental service building is shown in Figure 4. The general locations of the four experimental focii are indicated as well as the set-ups of four initial experiments. Provisions have been made for mounting four experiments simultaneously with sequential running envisioned. (Some parasite work is, of course, possible.)

The basic experimental area is 30' x 230'. The upstream one quarter of the area has a floor level of 730', as does the tunnel section, and the downstream section has a floor level of 727'. The high floor level in the upstream part was dictated by the need to allow for crane handling of items coming out of the upstream section, the desire to have a height identical to that of the high intensity proton target beam height for the upstream high intensity F1 target, and by the desire to minimize the shielding support problem around this same target. In addition, a corridor extends 74' downstream from the end of the experimental hall to encompass the equipment of an experimental 90° CMS spectrometer. The axis of this corridor lies at an effective angle of 79 mradians with respect to the secondary beam passing through the F1 target. There is complete 20-ton crane coverage over the entire 30' x 230' area.

As indicated in the plan view, each experiment has 800 square feet of work space in the experimental service building divided into an experiment electronics area and a work area with a movable wall between such that the ratio and arrangement is left to the individual experiments. Each electronics room is connected to the experimental area by a set of conduits for coaxial and ribbon cables. Every experiment has the normal committed controls console and crate in addition to its own electronics, and this is mounted in the electronics room.

The remaining space in the service building is equally divided between a cryogenics pump room, and a power supply room. The absence of a large LCW plant is due to the expected preponderance of cryogenic magnets in the area. Any need for LCW will be supplied from the large upstream plant. A total of 2150 square feet is allocated for these purposes, and the contents are discussed in the technical appendices.

Finally, the service building contains a two-ton lift for dropping small items of experimenters' gear into the experimental area. The major equipment access is an 11' x 29'4" drop with a shielding block hatch, which lies to the north of the service building. A 45-ton travel lift will provide the major equipment handling device both for the upstream access and the downstream service building. A steel floor is provided on which to roll the heavy equipment from the drop into the experimental area beneath the crane coverage.

Technical Appendices ■■■■■

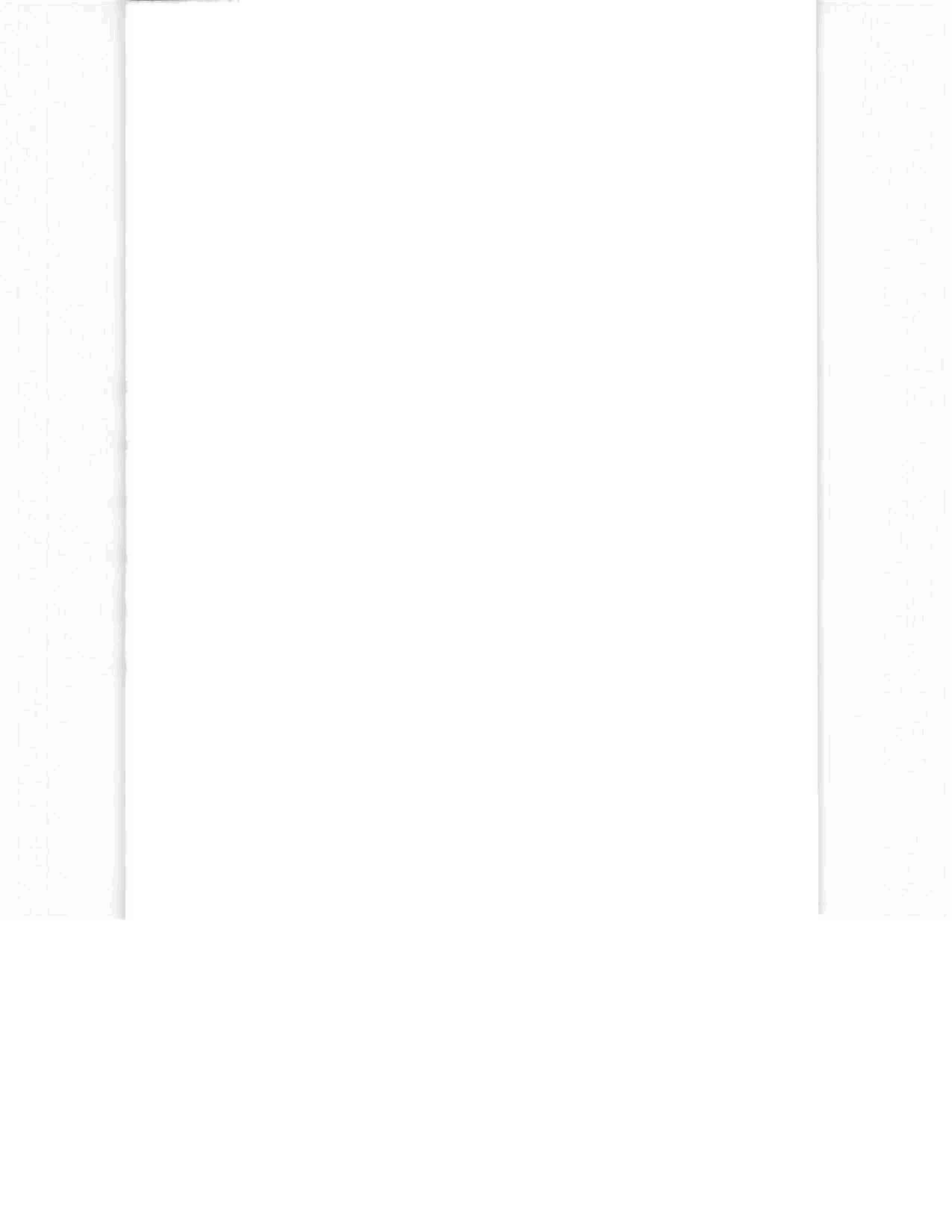
A. Radiation Safety ■■■■■

B. High Intensity Pion Cryogenic System ■■■■■

C. Electrical Design ■■■■■

D. Mechanical Design ■■■■■

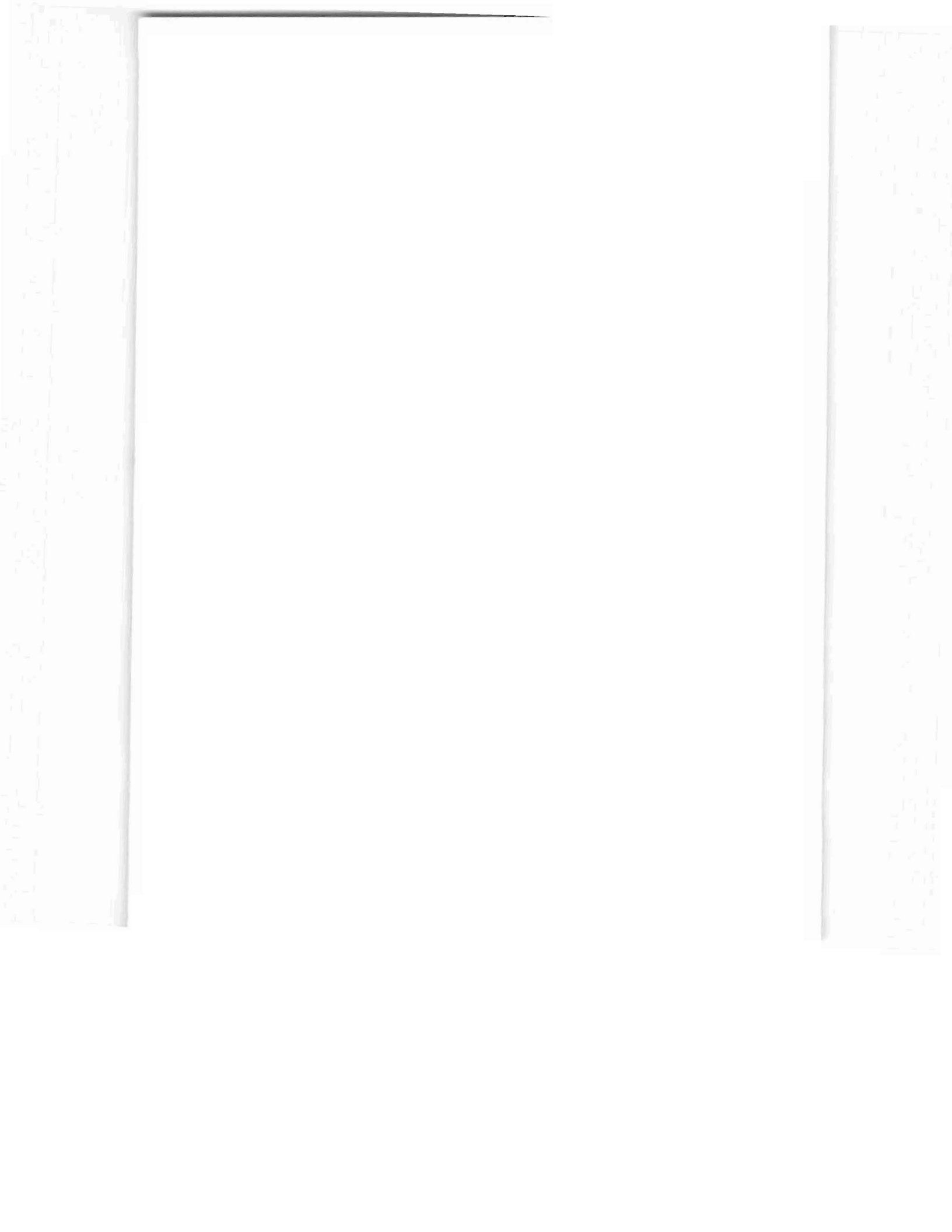
E. Instrumentation ■■■■■



Radiation Safety [REDACTED]



[REDACTED]



II. TECHNICAL APPENDICES

Appendix A: RADIATION SAFETY

The design criteria for this area includes the requirement that the targeting system be capable of handling 10^{14} protons/pulse (1 second of spill on an eight second cycle) because of the desire to produce the highest intensity secondary beams possible. This criterion places severe demands not only on the mechanical systems that must safely handle this much radiation (see Appendix D) but also requires massive shielding and procedural safety for the secondary beam area usually associated with a primary beam. In this section the shielding requirements are discussed from the triple standpoint of beam-on personnel safety outside the area, personnel protection from residual radiation during accesses to the area, and minimization of ground water activation. Personnel safety during actual handling of equipment associated with the target box is deferred to Appendix D. In addition, the interlock system is outlined and the safety of the area during the construction phase while experimentation is under way in the existing Proton West Area is discussed.

1. Shielding Calculations

The first point addressed in the consideration of the design of the targeting area was the restriction of limiting the number of interactions in uncontrolled soil to $.015 \times 10^{13}$ /second (with energy greater than 300 MeV).

An integration of the nuclear cascade results produced by the CASIM program yields the approximate form for a cylindrical steel absorber

$$S > R \equiv \text{total number of interactions (p > 300 MeV/c)} \\ \text{outside a radius R (R large) per interacting} \\ \text{proton} = 80e^{-.042R}$$

$$S > Z \equiv \text{total number of interactions (p > 300 MeV/c)} \\ \text{beyond the longitudinal distance Z (Z large)} \\ \text{per interacting proton} = 5300e^{-.0275Z}$$

Using .015, the rough conclusion is reached that $R \gtrsim 213$ cm of steel is required in the region of shower maximum and that $Z > 518$ cm is required in the 0° direction to contain secondaries produced by a flux of 10^{14} protons/8 seconds. More detailed considerations of the cascade profile using CASIM and the curves of Reference 1 have resulted in the target box construction discussed in Appendix D, and the exterior steel concrete sandwich discussed in Appendix E. The approximate conclusions are still basically adhered to in the final architectural design.

The second radiation safety requirement that has to be met is consideration for the safety of personnel during beam-off accesses to the hot areas. Worst-case estimates have been made of the residual activation levels of the sides of the target box immediately after turn off after infinite time of irradiation of the target box with the design goal of 10^{14} protons on an eight second

cycle. The following positions are listed:

West surface of target box	- vicinity of pretarget	- 20 mr at contact
West surface of target box	- vicinity of upstream end of dump	- 40 mr at contact
Downstream end of target box	- vicinity of 0°	- 90 mr at contact

The levels of activation of the downstream end of the target box are minimized by the addition of three feet of low activation concrete at the downstream end of the dump. The additional trick of Cd coating could cut these levels by a factor of 3.

The third requirement is that the target box and the surrounding earth of the berm be capable of protecting personnel from beam-on radiation. After degrading by a steel shield, such as incorporated in the target box, the flux emitted is attenuated by a factor of 10 for each four feet of light concrete. In the approximation that five feet of Fermilab soil is equivalent to four feet of light concrete for shielding purposes, twenty feet of earth berm is sufficient to limit the dose received by personnel engaged in activity directly over the enclosure to less than .1 mrad/hour.

This third requirement must be examined in the experimental area itself. Intense secondary beams of 10^{11} pions/pulse can result from the targeting of such an intense proton beam. For this reason and for the reason that it will be possible to target the proton beam in the experimental hall, it was desirable to place the experimental hall underground and thereby to shield as much as was economically feasible the rather exposed targeting locations F1, 2, 3, and 4, which are distributed along the enclosure as shown in Figure 4. Because of the large span (30') of the experimental hall, only five feet of berm could be placed on the top of the PW-5 enclosure. To limit levels in the adjacent counting rooms to 1 mr/hour, it may be necessary to shield locally each target and perhaps the transport line through the pit to the target with approximately 1.25 feet of steel on all sides.

The final problem that is examined in this section is the feasibility of dumping the proton beam in the downstream dump area of the existing P-West and allowing personnel access to either the experimental hall or the upstream target area (PW-3) of the High Intensity Laboratory. Since the worst problem with such a plan will be the radiation levels in PW-3, we have calculated the levels that we expect at the upstream end of PW-3 with various configurations of steel (see Figure 6b) and various angular deflections of the dumped proton beam. As shown in Figure 6a, if we reverse polarity of the safety bend and dump the protons with an angular deflection of greater than 10 mrad

then the intense muon cone misses the enclosure and the radiation levels in the enclosure are quite minimal. Even at 1000 GeV, the penetrating muons lead to levels below .1 mrem/hour/ 10^{12} protons/pulse. (See the 1000 GeV asymmetric triangular shield curve of Figure 6a.)

2. Interlock System

The existing P-West radiation interlock system remains intact with only minor modifications to accept the system used in the new area.

The new interlock system consists of three independently keyed areas having a common primary and secondary critical device. The primary critical device consists of the three "safety bend" dipoles at the downstream end of the existing P-West area. The secondary device is a collimator situated downstream of these safety bends which closes off the access to the 6" pipe connecting downstream P-West with PW-3, the proton targeting enclosure. If either the collimator fails to close or the safety bend does not have reverse current and is not deflecting the incident proton beam maximally to the east while access is being made to any part of the downstream secondary beam area, the present critical device for the entire P-West Area, MH321 in Enclosure H, will be tripped.

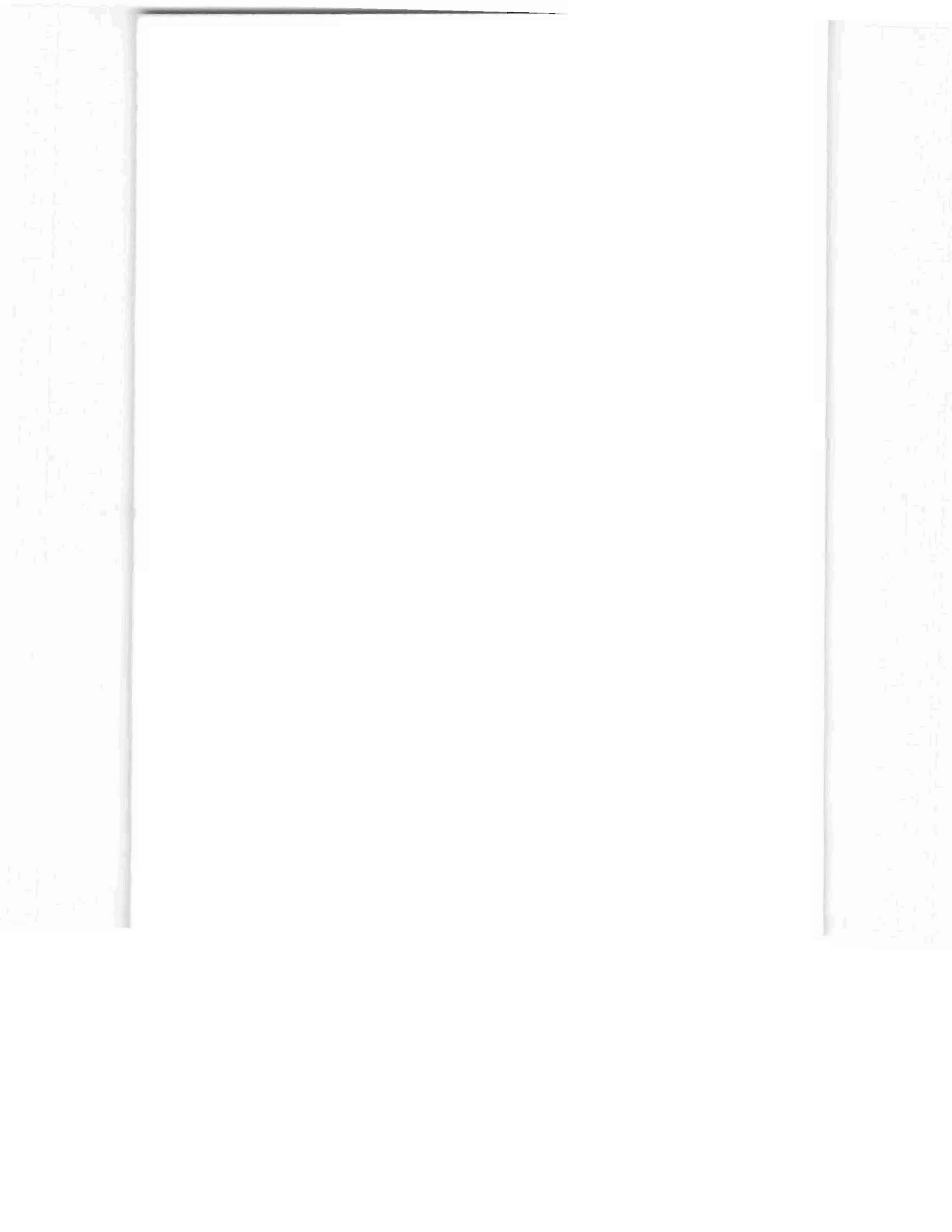
While the primary proton beam is deflected to the east and the collimator at the end of PW-2 shuts off the pipe to the high intensity area, the intent is that accesses be allowed into the area. To that end, a triangular steel shield has been designed to attenuate the high energy muon flux that would otherwise penetrate.

The three distinct areas with independent logic loops in the new high intensity are:

1. The proton targeting enclosure PW-3 and the momentum slit area PW-4.
2. The secondary transport tunnel.
3. The experimental hall PW-5.

Each of these areas can be searched and secured independently of the other areas. The key trees for each area and indications of the logic loop status will be centralized in the Pagoda in the standard way.

High Intensity Pion Cryogenic System ██████████



Appendix B: HIGH INTENSITY PION BEAM CRYOGENIC SYSTEM

a. Introduction

The installation of large numbers of superconducting bending and quadrupole magnets in the target, transfer, and experimental areas of the High Intensity installation require a rather large refrigeration system and a method of moving the liquid refrigerant to the magnets. The two plans considered were local refrigerators and power supplies, and centrally-located refrigerators and power supplies. The local refrigerator plan is very expensive and of little flexibility from a standpoint of shifting refrigeration from areas of low demand to those of high demand during operation. Because of lower cost, centrally located operation, and the refrigerators being located in the standard service buildings at the two ends of the line, the centrally-located system has been chosen.

This report addresses itself to the concept, design, and installation of the refrigerators, 2-phase liquid helium transfer, and the preferred philosophy of power distribution to the magnets.

b. Summary

The system has been designed using the following criteria.

1. The system must supply liquid helium and power to approximately 55 magnets distributed along a total length of 1000 feet divided into two sections - 500 feet upstream, and 500 feet downstream.
2. Depending on the type of magnets eventually built for the beam line, either high current (2500A), or low current (200A), must be supplied to energize the magnets. Designs are presented for both considerations.
3. The transfer line is located in the tunnel above the magnet line.
4. Thermal contraction of up to 22 inches must be accommodated within the helium conductor tube.
5. The system must be seated in a manner that allows removal and/or addition of magnets without the need to warm up the entire system.
6. The system will use two energy doubler satellite refrigerators - one located in the target area service building, the other located in the experimental service building. An inter-connection in the center will enable single system operation of helium transfer.
7. Power supplies must be so located as to permit hook-up

to the superconducting leads near the refrigerator system in the case of 2400 amp design. In the case of 200 amp magnet design, the power will be transported via conventional cables to lead boxes for individual magnet groups.

c. Refrigeration Load of the System

The magnets as presently designed will operate at 4.5°K with a helium vapor heat shield at ~ 80°K and super insulation in vacuum. The transfer line will also be shielded by helium vapor and super insulation in vacuum. The following summary of heat load is estimated.

	<u>4.5°K</u>	<u>80°K</u>
1. Magnets (55) 6 Watts Each	330 W	500 W
2. Transfer Line	50 W	290 W
3. Lead Contact Resistance	15 W	
4. Lead Cooling 7 - 2.4KA, 22-200A	45 W	
5. Helium Pump	35 W	
6. Miscellaneous	<u>25 W</u>	<u> </u>
	500 W	790 W
	700 l/hr	54 l/hr

One satellite refrigerator will be located in the target service building upstream, one located in the experimental service building downstream.

Each refrigerator will make 325 - 340 l/hr. The total of 650 to 680 l/hr is short of full load of 745 l/hr during 1000 GeV operation. Therefore, an additional supply of approximately 70 liters of liquid helium per hour will be required during 1000 GeV operation. For future experimental hall load, we might at this time consider a third satellite refrigerator to be located in the experimental service building.

d. Transfer Line (2400 Amp Design)

1. The design of a 2400 amp transfer line is similar to a two phase helium distributor system, with the power leads contained within and cooled by the one phase helium. See Figure 7.

The main section of the line is to consist of an outer tube 8 inches in diameter - at room temperature, hung in brackets above the magnet line. Within this outer tube is the 80°K heat shield supported by G10 spacers; within the heat shield is the 4.5°K single and two phase helium line which consists of two concentric tubes, the single being the inner, the

two phase flowing in the outer. The power conductors are laid in the inner tube.

Approximately every 50 feet, a junction box is located in the line to service magnets with refrigeration and power. See Figure 8.

2. Transfer Line Pipe Size (2400 Amp Design)

The single phase helium pipe size is basically controlled by the number of conductors within the line at any given point. It is desirable to keep the line as small as possible, to hold the helium inventory to within reasonable figures.

Helium flow rate of ~ 380 l/hr will result in a maximum flow in the single phase tube of 1.7 gal/minute. With the designed size of 2.5 inch diameter single phase line with seven 2400 amp and twenty-two 200 amp leads, whose total cross sectional area is 1.47 inches squared, the cross sectional area left for helium is at most 3.44 square inches. 1.7 gal/minute liquid velocity through a pipe of 3.44 square inches is approximately 0.162 feet/second. Flow in the two phase tube is sized to handle the flow at the same rate as the single phase.

To cut down on the helium inventory, the pipe sizes will decrease as the number of conductors decrease within the line, as well as the number of magnets being refrigerated. The liquid helium inventory will be on the order of 900 gallons for the entire system; magnets, lead box, and storage.

3. Refrigeration Control

Due to the large number of leads and separate parallel helium paths, flow control is needed to ensure each magnet and system section proper cooling. To do this a pump is used to move the liquid helium in the system; each magnet string will then control its own flow rate by means of an expansion valve between the single phase and two phase systems. The expansion valve will receive a temperature signal from a sensor located just before the expansion valve on the single phase side. An expansion valve will also be located at the end of the transfer line to keep the single phase system stable within the transfer line. See Figure 9.

e. Transfer Line (200 Amp Design)

1. The design of a 200 amp transfer line would be a single pass liquid helium line with a cold gas return. See Figure 10. The main section of the line is an inner stainless steel tube on the liquid side, and a stainless steel tube for the cold gas return. The cold liquid and gas tubes are enclosed in an 80°K heat shield and super insulation in vacuum. Contraction of the cold tubes is taken up in nesting type bellows.

2. Transfer Line Tube Sizes (200 Amp Design)

Since there are no conductors in the 200 amp design, the only requirements are helium flow.

The basic flow rate of 380 liters/hour of helium remains unchanged for either system, therefore, the rate of 1.7 gal/minute as stated in Section d.2 remains true. Since the maximum flow rate for helium is quite high, a rather small tube size can be used. Five-eighths (5/8") inch diameter has been chosen which will give a flow rate of approximately 1.2 ft/second. A cold gas return tube of one inch diameter will be used. The outer vacuum jacket of three and one-half inches (3-1/2") will be at ambient temperature. The liquid helium inventory with the 200 amp system transfer line will be approximately 700 gallons for the entire system.

f. Satellite Refrigerator

The refrigerator is the Energy Doubler satellite station design. This unit is basically self-controlled. The control system consists of pneumatic readout vapor bulbs.

The services to the refrigerator consist of 275 KVA of power, and 50 GPM of cooling water.

g. Cryogenic Design of the Magnet

The basic cryogenic system of the magnet design has been established. This consists of a central cold bore tube inside the coil package. Outside of the coil package is a double wall cryostat.

The single phase helium liquid fills the inner chamber and coil package; the two phase helium fills the cryostat wall. The shield wall is cooled to approximately 20°K. Interconnection between magnets is made within a vacuum pipe which carries the two helium lines plus the power leads. See Figure 11. At this time, the current requirements of each type of magnet is undetermined.

Electrical Design 



Appendix C: ELECTRICAL DESIGN

The electrical design can be divided into two sections, as follows:

The DC equipment for beam line magnets.

The AC distribution system for conventional loads such as building services, pumps, compressors, etc.

a. The DC System

The design for the DC system is governed by the AC supply voltage and load requirements. In general, we will have a highly current regulated AC to DC power supply feeding the load. This power supply will be constructed in such a way that it can be operated and monitored from Fermilab's standard computer system. The AC input side will be fed from the standard 480V, 3-phase, 60 Hz secondary distribution system. The output of the power supply will use a 6-phase rectifier system, with either primary or secondary control. The power supply will not use power filters at the output but will have freewheeling diodes for protection and ripple reduction at reduced output voltages. In addition, we will use a manual tap changing mechanism to make the units more universal for different operating voltages. A quenching circuit, which consists of a solid state switch, a resistor, and associated electronics will be installed as an integral part of the power supply. A short discussion of the quenching circuit follows at the end of this section.

The magnet design is indefinite but there appear to be two likely designs, as follows:

1. a 3000A, 0.35H magnet, and
2. a 300A, 35H magnet.

The 3000A magnets will be fed via a cryogenic transfer line and this system therefore requires very low power supply output voltages. The 3000A power supply will have an output rating of 0 to 4 volts, but can provide a 10 volt output for short periods of time. This higher output voltage makes it possible to reduce the charging time to about 60 seconds. Because of the low DC output voltage, the 3000A power supply will use primary control and circuitry for AC power factor correction.

The 300A magnets will be fed via conventional cross linked polyethylene cables about 1000 feet long and will require therefore a higher output voltage at the power supply. The 300A power supply will have an output voltage of 0 to 30 VDC, which results in a charging time of about 16 seconds. Because of the higher output voltages, the 300A power supply will use secondary control for regulation.

The Quenching Circuit

The goal of the quenching circuit is to limit the amount of stored magnetic energy that is dissipated into heat in a magnet that has gone normal. This can be done by inverting the power supply or by switching a resistor in series with the magnet as soon as a quench begins to develop. Inverting the power supply is not practical because of the low rated power supply output voltage and also because of diodes at the power supply output side. Switching in a series resistor is the most practical solution. Switching can be done fast (approximately 100 μ sec) if a solid state switch is used. The value of the series resistor determines how fast the current will decay toward zero, and how large a fraction of the stored energy is dissipated outside. Larger values of the series resistor cause faster current decay and a larger fraction of stored energy dissipation outside. However, large values of the series resistor also cause high system voltages, which may lead to magnet breakdown. It is reasonable to select the series resistor such that the maximum voltage across it is in the order of 100V to 200V. Figure 12 shows in principle how a quenching switch would work.

The first thing to do is to detect a quench and ride through magnet $L \frac{di}{dt}$ voltages during startup, while the quenching detector is always active. An elegant solution for this is to bring a wire from the center of the coil and form a Wheatstone bridge by installing two external resistors. The Wheatstone bridge is insensitive to frequency and will only produce an unbalance voltage if the coil halves change independently. The unbalance voltage is amplified and

1. triggers the commutating SCR,
2. blocks the power supply SCRs,
3. trips the power supply contactor, and
4. removes the series SCRs gate.

Upon firing of the commutating SCR, the charge of C_1 is released into the load loop and effectively reverse biases the series SCRs for a period longer than their rated turn of time. After the series SCRs are off, the magnet current charges C_2 until the voltage across C_2 equals the voltage across the series resistor. At that time the commutating SCR shuts off by itself, because the commutating power supply is current limited to a value lower than the minimum holding current of the commutating SCR. The capacitance values of C_1 and C_2 are rather large (order of 6000 μ F for a 3000A switch) and need therefore to be built from good grade electrolytic capacitors for reasons of economy and size. Several units should be operated in parallel to limit the current per can to less than 1000A peak. Higher currents per can will lead to premature failures

due to foil and tab burning. We would need only one capacitor bank, without capacitor bypass diodes, if a non-polarized (extended foil/paper) capacitor were used. However, the size and price are prohibitive. The capacitor bypass diodes prevent reverse biasing of the polarized units.

When a string of superconducting magnets is operated in series, it might be justified to install bypass SCRs in parallel with each magnet. These SCRs are normally off, but when a magnet in the string turns normal, its bypass SCR gets fired on, providing a bypass for the stored energy current from other series connected magnets. Turn on of these SCRs will only work when the magnet terminal voltage exceeds about 2 volts.

b. DC DISTRIBUTION SYSTEM

Power Distribution and Loads (See Figure 13)

To bring electrical distribution to the high intensity area, the two existing Proton Lab high voltage feeders, 36 and 37, must be tapped and stepped down 13.8 kv to 480 v at unit substations in the vicinity of the two service buildings. From the substations, power is then brought into the buildings to switchboards and motor control centers to provide power for power supplies, mechanical equipment, and utility purposes.

In order to extend Proton Lab 13.8 kv feeders 36 and 37 to the Pion Area, a duct bank is required approximately 120' to the pad for the target service building, and approximately 720' north to the substations at the Experimental Hall.

The feeders will be spliced into at existing Manhole P137, pulled through an existing section of duct bank along Batavia Road, and branched to the two service buildings from Manhole P137B through the new ducts.

The two service buildings will also be linked by a bank of communications ducts placed parallel to and built at the same time as the power duct extension.

At both buildings, the incoming feeders will terminate in oil switches on the concrete pad with the substations which they will energize.

A full connected load inventory (Table IV) shows a requirement of 2.1 MVA for the target service building, and 3.0 MVA for the Experimental Hall. The need for additional power in P-Center and EE4 justifies the need for two 1.5 MVA substations at the P3 Service Building.

Secondary Distribution

From the air circuit breakers at the unit substations, a feed is to be brought into the building for a 2000A switchboard and a feed for the motor control center.

While initial load requirements at the Target Service Building presently require only one 2000A switchboard, two are necessary at the Experimental Hall Area. From these switchboards, power will be supplied to conventional 500 kw Transrex rectifiers and to subpanels for cryogenic supplies. These subpanels were chosen because they appear to be the most economical way of providing a large number of circuits of lower current rating (60A). They also incorporate the features of having lockouts and being fusible.

A system of cable trays as shown on the drawings, differs from the other Proton Lab Areas in that the DC current supplied to the magnets flange (> 2000 amp) will flow through cryogenic transfer lines. Therefore, the amount of tray required for heavy DC cabling is substantially reduced. The number of penetrations is also much reduced. These penetrations are used mainly for signal cables since the DC power distribution is minimal in any circumstance.

Utility power throughout the buildings and belowground tunnels originate from 480V panels appropriately placed for use in illumination, sump pumps, welding outlets, etc. The areas will also be served locally by small (30 KVA) dry type stepdown transformers and panels providing 120/208V for appliance power. The Experimental Hall compartments will each contain their own 30 KVA transformer and 100A panel for 120V individual circuit distribution to each relay rack for instrumentation power.

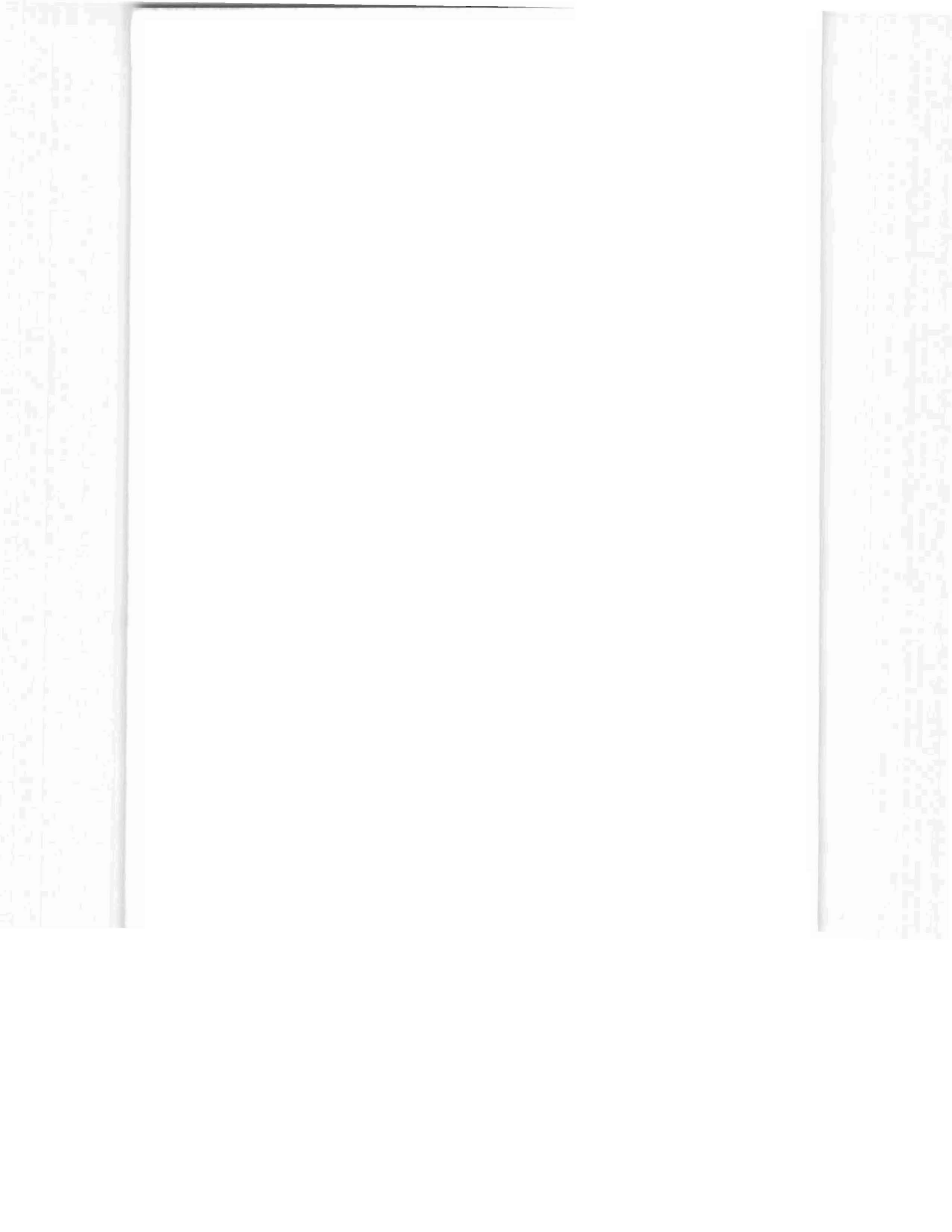
Motor Control Center

Power from the unit substations will also be brought into the mechanical equipment rooms of each service building to a Motor Control Center. These will consist of unit assembly, multi-bay systems of combination starter cubicles. The sumps for the water systems will have combinations of molded case breaker, contactor, and thermal overload. In some instances, where elements of the refrigeration system already contain their own contactor, only a molded case breaker will be necessary. Each appropriately sized starter will contain its own control power transformer selector switch for manual or pilot device operation, and two sets each of N.O. and N.C. auxiliary contacts for monitoring and interlock.

A monitoring system for the water system has been devised consisting of temperature, level, and conductivity sensors brought out to a chassis from which signals may be used for alarm and control of mechanical devices. Also planned is the use of an electrically powered makeup water valve and a pneumatic device to control the cycling of the cooling towers.

Signals from this chassis may be transmitted on the 'mini' digitizer or by cable to the Pagoda. A similar monitoring system is also being considered for the satellite refrigeration stations.

Mechanical Design 



Appendix D: MECHANICAL DESIGN

1. Target Box Design

The basic target box components consist of a beryllium target assembly, a main ring B2 dipole magnet, a collimator and dump assembly, and all of the associated shielding. The general philosophy of this target box design (shown in Figure 14) is predicated on the necessity of avoiding moving any component of the target box that does not have to be moved. Accordingly, each of its major elements can be extracted without disturbing the other elements or the cryogenic magnets upstream and downstream of the target box. Given the radiation levels expected (see Appendix A), special attention must be given to methods of shielding, access, remote service connections, and to backup systems or alternative methods of servicing the components if failures occur.

The target is a water-cooled beryllium rod 1.5" in diameter and 12" long, pressure fitted in a copper jacket, as shown in Figure 15. This target assembly can be removed separately with or without the 2' x 2' x 6' water-cooled steel envelope that houses the cylindrical copper jacket. The extraction process takes place from the upstream end and is designed to avoid the necessity of moving the superconducting dipole situated in front of the target box. The entire assembly on the cylindrical copper container extracts into a relatively small lead box for moving or storage. Because of the activation levels expected and the desire to keep the assembly simple, the target is stationary with no complex mechanical motion built in, and is somewhat larger in size than necessary in order to be adequate for all targeting configurations of the proton beam (see Figure 2a). Because of the contamination, water degradation, and the beam load, the target assembly, like the rest of the target box equipment, will require cooling by a closed loop LCW system (see Appendix D.4). Since the beryllium target is large, the surveyed location of the target is relatively unimportant ($\Delta x, \Delta y \sim \pm .1"$). The axial position of the target also requires little setting precision ($\Delta z = \pm .25"$).

The B2 sweeping magnet located immediately downstream of the beryllium target assembly, as shown in Figure 14, is a standard main ring dipole modified only in its service connections and manner of support. The collimation system just downstream of the beryllium target shadows the B2 aperture from a direct view of the target and prevents accidental deflection of the primary proton beam into the coils. This is required since the B2 is the most fragile component of the targeting system. The design of the shielding around the B2, shown in Figure 14, is complex because of the necessity of extracting the B2 in case of failure transverse to the beam. As indicated in Figure 14, the 'Egyptian' shielding wall will be raised by

four 100-ton jacks situated at either end of the space occupied by the B2. This arrangement allows the removal of the B2 without disturbing the collimator/dump or the target assembly which are expected to be activated to 500 rad level. The services, both power and water, for the magnets are introduced from above the shielding and are designed for remote removal even if current welding occurs at the 5000 amp junction.

The third major component of the target box is the downstream collimator/dump. The construction of this dump to withstand the thermal stresses and heating arising from a 10^{14} proton/pulse beam is complicated and is discussed in the second section of this mechanical design report. As well as performing a function as a beam dump, this device performs the function of collimating the secondary flux. This collimator is cooled with the same chiller system which provides closed loop LCW for the target assembly and the B2 magnet. As shown in Figure 16, this dump/collimator assembly consists of 5 feet of aluminum and 17 feet of steel with a spiral copper tube cooling system coiled as close to the B2 aperture as mechanically possible without actually lowering the longitudinal density of material that obstructs the path of the proton beam. To avoid leaks, the cooling paths are continuous tubes with all manifolding at the rear of the target box. The approximately conical collimator apparatus shown in Figure 2b is constructed by boring consecutively larger diameter holes from the upstream to downstream end of the collimator on a common center line which is tilted at 4.01 mradians (to take into account the deflection of the beam by the B2) with respect to the 0° incident proton beam. The aperture can be varied from 1.85 mradians to .75 mradians by appropriate inserts which can be introduced from the downstream end of the target box. The horizontal and vertical alignment tolerances are approximately .020 inches.

2. Beam Dump

The desirability of operating the High Intensity Area with a 10^{14} pp slow spill makes the design of the collimator/dump difficult. The size of the proton beam as it impinges on the upstream surface of the dump (shown in Figure 16) in the targeting arrangements, schematically indicated in Figure 2b, can be calculated from the proton beam parameters given in the first section of this report. Using the spot sizes and divergences listed there, the cross-sectional area of the beam at the dump is approximately .5 cm². If the assumption that the production angle and B2 sweeping disperses the secondaries produced by 10^{14} protons interacting in the Be target enough so that they can be neglected in calculating the total energy dump due to the proton beam, the beam dump still must handle the beam power due to 3×10^{13} 500 GeV protons during a 10 second cycle (DC power of 800 kw). To accommodate this DC load, the chiller system has been sized to provide 100 gpm cooling to the sum of the upstream, target box and momentum slit. The proportion of the flow will be adjusted by the temperature of the return LCW lines. This cooling is more than adequate if temperature rises of 50° are allowed.

The much more serious problem is of course the instantaneous temperature rise in the small area in which the proton beam is dumped, due to the peak power dump of 8 megawatts. Because of the high radiation levels which will be present in the dump area a mechanically solid system is desirable. A competing system consisting of Al bearings coated to prevent Al hydroxide formation and immersed directly in the chilled water was considered because of its better heat transfer properties but was rejected because of the increased weld joints necessary and the overall lowered density of the dump. It was felt to be mechanically much more prone to leaks than the system described below.

The final system consists of a segmented solid beam dump cooled by a continuous copper tubing matrix imbedded in the material of the beam dump either by casting or compression fitting. The matrix of tubing within this beam dump is drawn in as close as possible to the region of the dump in which the proton beam is expected to impact and generate a hot cone. As shown in Figure 2b, this dump consists of an initial five feet of Al followed by 17 feet of steel and 3 feet of concrete. The energy density contours are shown in Figure 2c. As indicated there the Al serves as a relatively high heat transfer medium of low density which serves to shield the bulk of the dump which is composed of iron. In spite of this shield the energy density is highest at the front surface of the iron and therefore the greatest problems are encountered there.

If we assume the cone of the hadron shower can be approximated by a 24 cm radius cylinder by taking into account an average thermal diffusion distance during spill of 2 cm and a beam spot of .4 cm radius then the energy density as read from the curves in the center of the Al block is as an upper limit

$$\frac{dE}{dV} \sim .02 \text{ GeV/cm}^3/\text{proton}$$

For 10^{14} protons this corresponds to a density of 320 joule/cm³ or a calorie increase of ~ 8 cal./cm³. This for Al is a temperature pulse ΔT of 160°C. Since the pulse stress coefficient of Al is 250 psi/°C the developed thermal stress from this temperature rise is 40 kpsi which is approaching the ultimate tensile strength.

Using the curves shown in Figure 2c and taking into account that the thermal diffusion time in iron is approximately .8 cm/sec., an energy density ~ 5 times as great as that in the Al is expected. This leads to a

$$\frac{dE}{dV} \sim .1 \text{ GeV/cm}^3/\text{proton}$$

and a ΔT of approximately 200°C. The stresses developed in the iron are 70 kpsi, well within the ultimate strength of steel.

The conclusion is that the segmented Al-steel dump can handle albeit with difficulty both the DC and pulsed loads of the 10^{14} ppp design goal. By far the most serious problem is the thermal working of the various components under the instantaneous loads. Because of these instantaneous thermal loads, we have tried, as shown in Figure 16, to place the helical cooling tubes within a few thermal diffusion lengths of the beam impact point to attempt within-spill cooling.

3. Momentum Slit

The momentum slit must perform the dual function of defining the momentum bite of the secondary beam and of acting as a primary beam dump area since for a tune of positives the proton beam exits the target box area, passes through the first dispersing bend and impacts on the east side momentum slit. The slit therefore must be designed with the care that was taken with the collimator/dump. The general features of this design are shown in Figure 18. The same 100 gpm flow is provided for through unjointed copper tubes embedded in each jaw of the momentum slit. The first five feet of each jaw includes a 4" x 4" aluminum insert which is in contact with the cooling, and the remaining fifteen feet is steel. This slit is closed symmetrically about the beam direction by a motorized screw assembly shown in Figure 17, which is seated at the upstream and downstream end of the momentum slit and is far removed from the beam. All water connections are made at the downstream end of the slit.

As will be discussed in the transporter section of this report, the momentum slit can be extracted from the upstream end into the transporter. This is possible because of the absence of superconducting magnets on the upstream side of the momentum slit shielding pile. Provisions have been made in the design for a sliding Pb shutter to provide shielding from the upstream surface of the slit which will experience extensive activation during any extensive running of positive secondaries.

4. Transporter Design

The basic device used for removing components from the target box area and the momentum slit is a Pb walled (3" thick) transporter of the general mechanical design shown in Figure 10. The center of the container space is 36" above floor level and the interior volume of the container space is 24" x 24" x 30'. Total weight of this device when loaded with the dump is 43 tons. The 3/8" steel floor in the vicinity of the target box and magnet slit has adequate load bearing capabilities to support such weight. This transporter is designed to handle the B2 collimator/dump or the momentum slit assembly in case of failure, with a minimal dose to operating personnel. It is estimated, in the case of a dump failure after maximum exposure with a reasonable cool down time, that the entire operation of extraction and replacement would give a total dose of less than 300 mrad to the mechanical crew. This transporter can be loaded from the side with the dump/collimator or B2 magnet, or from the end with the momentum slit. In all cases, the operation of extraction and injection of these

elements is done remotely and provisions have been made to make blind connections of the extraction mechanism without exposure of the crew at any time to direct line of sight exposure to the elements. In all cases, more than adequate load bearing capabilities are built into the roller systems to avoid jamming or binding. In each case a manual backup method of extracting these components, which avoids direct exposure, has been provided for in the circumstance of such a failure of the primary extraction mechanisms.

The sequence of steps which would be followed in removal of a hot element from the target box begins with the longitudinal positioning of the transporter for extraction of the B2 magnet or dump/collimator. After the positioning of the transporter along the beam direction, the 90° set of wheels is jacked down and the weight of the transporter supported on them. The transporter is then pulled into contact with the Egyptian wall and the Pb side wall of the transporter is pinned to the steel shielding and is raised with that shielding when the 100-ton jacks are energized. At no time are the hot objects inside the shielding exposed. Two 7-foot screw and guide mechanisms with a twist locking connection are inserted through the other side wall of the transporter and are driven in and locked into the bedplate on which the magnet or dump/collimator is seated. After the connection is made, the screw jack drive is reversed and the magnet or dump is pulled to the west into the transporter, the sequence of steps reversed, and the transporter closed and pulled under the south drop hatch and removed by a travel lift. Finally, if the area has operated at full intensity for any length of time, the philosophy will be to discard the failed object without any repair attempt.

Accordingly, the transporter has been designed so that the Pb container can be removed from the undercarriage and discarded as a unit, thereby providing shielding in the radioactive waste storage area for the failed component. The 45-ton travel lift will form the main lifting device both for the targeting area and the experimental hall and will be adequate for lifting and transporting the expected loads.

5. LCW System (See Figure 19)

Consider a single location system in the P3 Service Building to handle three loads; 1000 kw in the target area, 400 kw in the experimental hall, and 550 kw cryo compressor cooling.

The target system would be a pure water loop located in the target enclosure area, cooling the high radiation load. This water loop will transfer the heat load through a tube and shell heat exchanger, in turn cooled by a glycol loop at ~ 42°F from two 150-ton refrigerant liquid chillers located in the service building.

Three Portor-Marlo type air cooled towers will supply cooling to the condenser side of the refrigerant chiller located in the target service building and also to the experimental hall in the form of low conductivity glycol solution, through 3-inch copper mains running the length of the beam enclosure. Pumps on the tower loop are two 100 hp units, to be run singly or in parallel. The following load breakdown shows that three towers will be required.

1. The Target Area Station is a 1000 kw load, which requires 286 tons of refrigeration.

Two F-22, 150-ton chillers cool the heat exchanger glycol loop to $\sim 42^{\circ}\text{F}$, which in turn cools the LCW (pure water) loop to the target area.

2. The total load has the following components

Total Load	1000 kw
Chiller Load	300 kw
Experimental Load	400 kw
Cryo Compressors	550 kw
Pumps	<u>75 kw</u>
Total Load	2325 kw

A tower will handle $57200 \text{ BTU/hr}/^{\circ}\text{FAT}$, or 836 kw at a temperature difference of 50°F . Therefore, three towers are needed.

The low conductivity water system will supply cooling to the target system at 200 gpm @ 200 psi. This will result in an approximate 35°F temperature rise in the water return. At 75°F supply, the operating temperature is 110°F , well within the safe operating range of the system.

Pumps will be bronze cased, centrifugal type, two pumps, 10 hp each on the chilled glycol side, one each for operation, one each for 100% standby. In the event that higher loads are used, the pumps may be run in parallel.

Copper pipe will be used throughout the system, and 4-inch mains will supply cooling to the target area. Since one major unit, dump, collimator or momentum slit will be required to take the 1000 kw load at any one time, each unit will take its cooling from the 4-inch main through temperature controlled flow regulator valves located in the return lines, each of the three units will receive one-third of the total flow for steady state conditions. The regulator will monitor the flow temperatures; upon a temperature rise in any one unit, the control valves will shift flows, holding $\sim 40^{\circ}\text{F}$ across the unit calling for the additional cooling. In this way the unit needing the 170 gpm at full load will be able to be cooled even though the total supply is only 200 gpm.

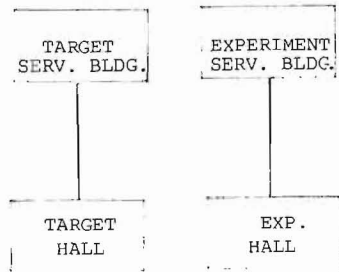
3. For the 400 kw load of the downstream experimental area, 100 gpm low conductivity glycol solution from the towers will be taken through the beam enclosures in 3-inch copper mains. The operating temperature will be on the order of 75°F to 95°F supply, 115°F to 140°F return.
4. Cryo compressor cooling: 100 gpm low conductivity from the tower system will cool the compressors in the target service building and the experimental service building.

We compare in Plan 1 the costs of a double size system in which closed loop chillers are placed in both P-3 and P-4. In Plan 2, which is preferred for cost reasons and has been adopted, we have closed loop chilled water available only in P-3 and supply ordinary LCW to the experimental area via piping down the beam tunnel.

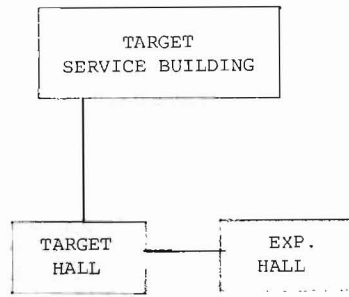
Although the installation of Plan 2 is some \$8400.00 greater than Plan 1B, it is felt that the greater savings in system operation and maintenance will offset the cost difference.

A cost breakdown for each considered system is as follows.

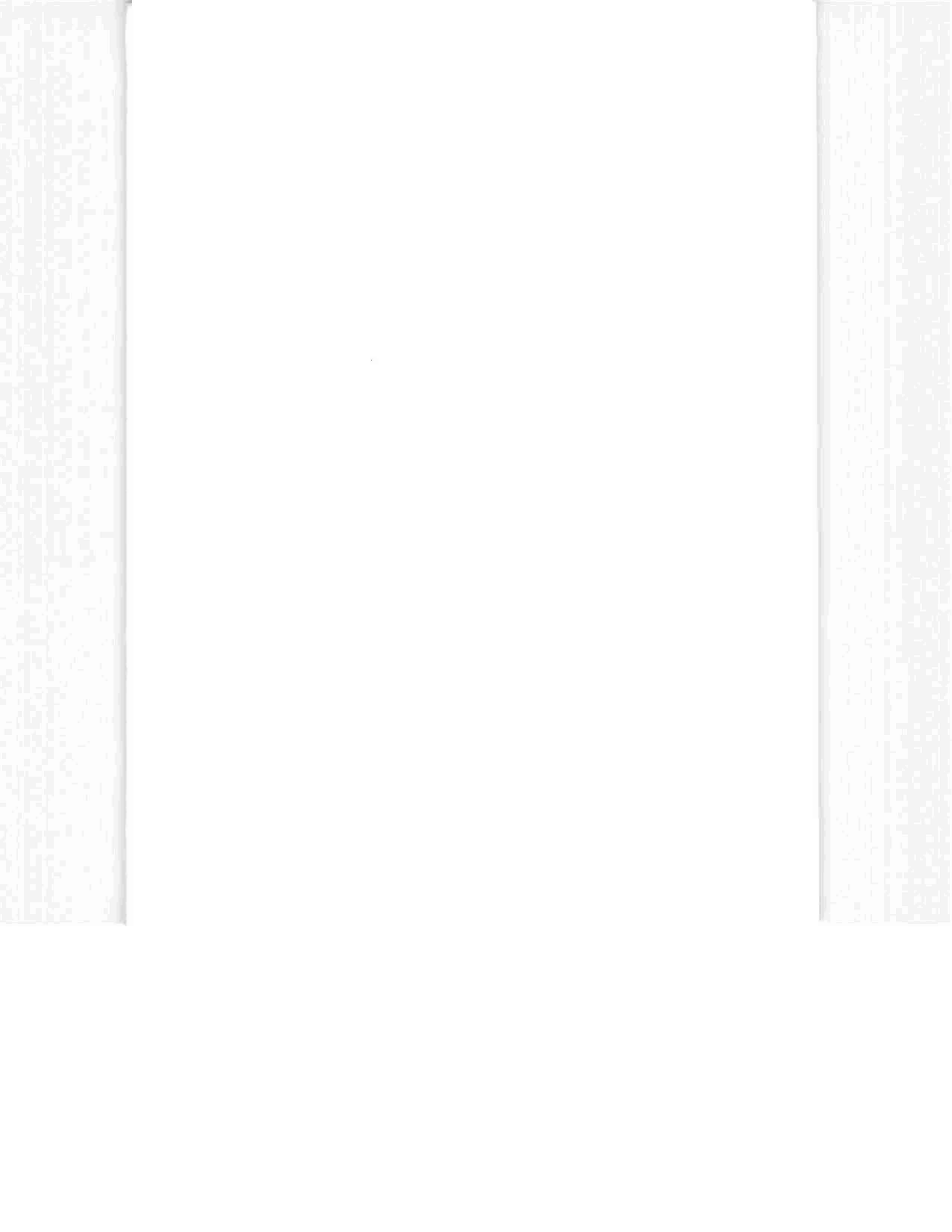
PION SYSTEM COOLING:	PLAN 1		PLAN 2
	<u>A</u> 1500 KW	<u>B</u> 750 KW	750 KW
Chillers	22,000	11,000	11,000
Chiller Fan Units	32,000	16,000	-
Air Cooled Towers	18,000	18,000	36,000
Glycol Pumps	24,000	13,000	14,000
LCW Pumps	7,200	7,200	7,200
Chiller Pumps	3,500	3,500	3,500
Labor	18,000	18,000	15,000
Pipe Runs - Pipe & Labor	<u>6,000</u>	<u>6,000</u>	<u>14,400</u>
	\$130,700	\$92,700	\$101,100



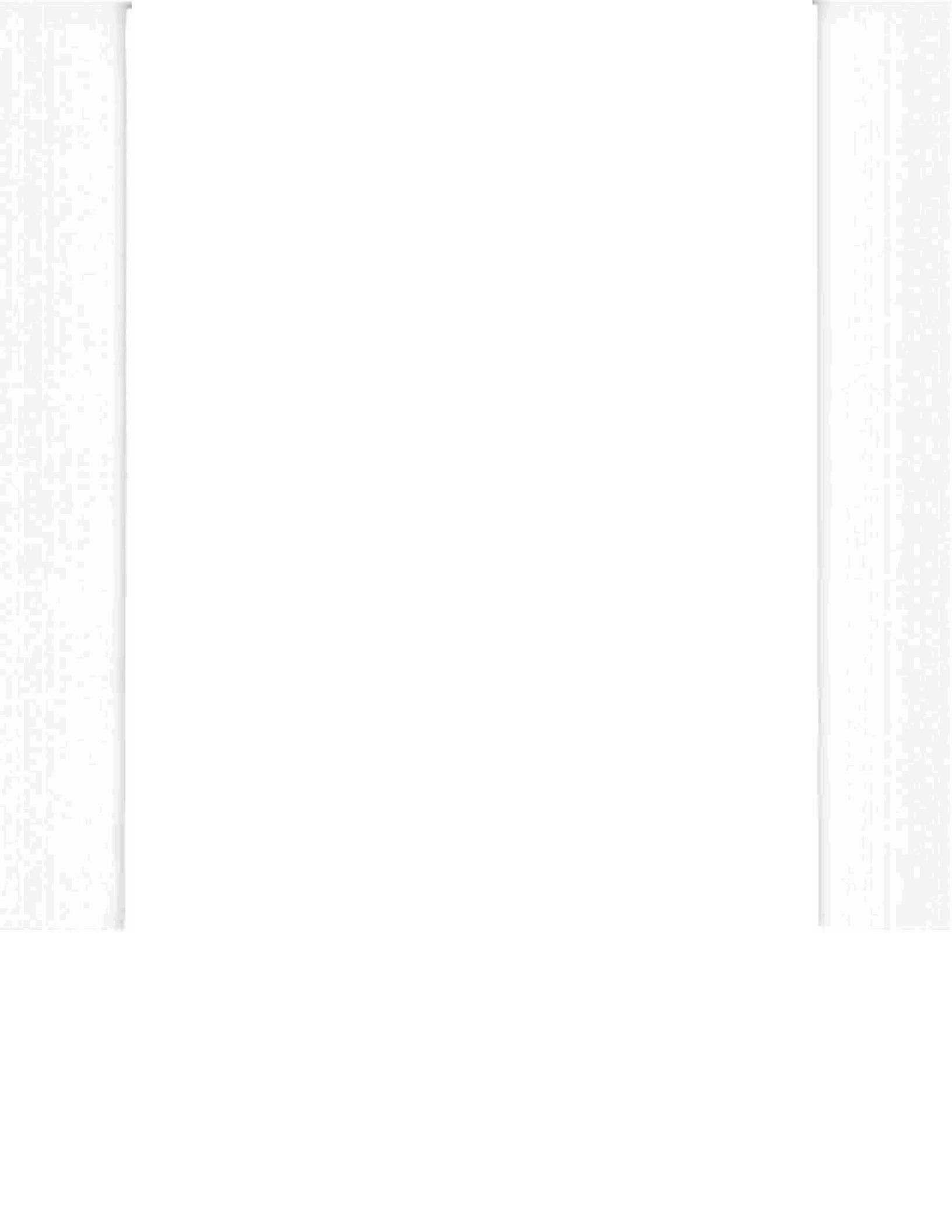
PLAN 1



PLAN 2



Instrumentation 



Appendix E: INSTRUMENTATION

This appendix contains discussion of the proposed instrumentation for the P-West High Intensity Secondary Beam. Pion beam intensity is expected to be between 10^6 and 10^{11} per pulse. However, lower beam intensities may be expected for anti-proton fluxes as well as during initial tuning for the pion beams. Instrumentation capable of handling this broad range of intensity presents some problems. Although most of the instrumentation will be standard when compared to other areas, some new devices will have to be developed to cover the cryogenics systems and low beam intensities.

Beam Line Instrumentation

A total of nine SWICs is proposed. Two are located prior to the beryllium target, and seven beyond the target. The location of each SWIC, numbered one through nine, is shown in Table V. Conventional SWIC manipulators can be used since liquid helium transport lines can be carried from magnet to magnet around the SWICs and/or other instrumentation required to be in the beam path. The type of SWICs needed was determined subject to the following assumptions.

1. Each particle passing through the chamber generates a primary ionization of 50 ion-electron pairs per plane (.25" between signal and HV planes).
2. 0.01 μ f capacitors are used to collect the charge (Ci).
3. A signal of 100 mv (Vc) is desired on the collecting capacitor corresponding to the peak signal wire.
4. Each wire collects all the charge due to particles passing 1/2 the wire spacing on either side of the wire.

Definitions

- G - Chamber gain - ratio of total charge collected to that created by primary ionization.
- q_i - Total charge collected on wire i.
- A - Scanner gain.
- N_i - Number of particles passing within 1/2 the wire spacing on either side of wire i.
- I - Beam intensity per pulse.

Hence,

$$V_c = \frac{q_i}{C_i} = \frac{1}{C_i} (50 N_i G (1.6 \times 10^{-19})).$$

For $V_c = 100$ mv and $C = .01$ μ fd solving for G yields

$$G = \frac{100 \times 10^{-3} \times .01 \times 10^{-6}}{50 \times 1.6 \times 10^{-10} \times N_i} = \frac{1.25 \times 10^8}{N_i} .$$

The expected beam profile beyond the beryllium target has been calculated by TRANSPORT and TURTLE and is shown in Figure 1 and tabulated in Table V at the proposed SWIC locations. From this data a resolution for each SWIC was selected and a value of N_{ipk} (corresponding to the peak signal wire) was calculated for both X and Y profiles based on the selected resolution. The minimum value of N_{ipk} from Table V is .054 I. Hence, the maximum required chamber gain would be

$$G_{\max} = \frac{1.25 \times 10^8}{.054 I_{\min}} = \frac{2.3 \times 10^9}{I_{\min}}$$

For beam intensities of 10^6 , G_{\max} would be 2.3×10^3 and type D-G chambers would be adequate. However, if an anti-proton beam is run, the intensity could be much lower. For this reason, it would be desirable to use type A chambers which have maximum gains of 10^6 and would meet the above signal criteria for intensities as low as 2.3×10^3 . Although type A chambers are best suited for the lower intensities, they are suspected of having a failure problem at high intensities which must be considered. A new NIM packaged scanner is being designed which would yield an overall factor of 10 increase in sensitivity and should help the signal to noise ratio of these devices. Type D1-G and D.5 are proposed for SWICs No. 1 and No. 2 respectively, prior to the target where there is a higher intensity proton beam.

A total of eight loss monitors are proposed for the pion beam. Although conventional loss monitors will be adequate at high intensities, an alternate will have to be developed to cover the low intensities. In addition, the desire to keep the ionization loss in the superconducting magnets below the nominal 10^7 minimum ionizing/cm³ level to prevent magnet quench problems makes higher sensitivity loss monitors more desirable. At present, typical loss monitor integrating capacitors collect 1 μ c of charge (1 volt per 1 μ fd) in P-East for 10^{10} lost particles/pulse. If the same sort of detectors are used and the sensitivity of integrators increased by lowering the value of integrating capacitor from 1 μ fd to 10 nfd and minimum count displayed kept about 100 (100 mv), the minimum collected charge would be 1 nc. This sensitivity is barely adequate to measure a "safe" loss. However, the observation is geometry-dependent since 10 μ c was collected from a loss monitor in P-West attached to a closed collimator receiving 10^{10} particles/pulse. Extrapolating, 1 nc would correspond to actual losses of 10^6 particles/pulse, which is in disagreement with that above by

a factor of 10. In any event, if the minimum collected charge is limited to 1 nc, we would probably not be able to set safe running conditions for the superconducting magnets using the current loss monitor system.*

If standard loss monitors are used, a new integrating scheme will have to be used to detect reliably 10 pc of charge.

An alternate to using standard loss monitors might be to use a Geiger tube or scintillator with phototubes. Both devices have the requisite sensitivity but are relatively more costly.

Cryogenic Instrumentation

It is not clear at this point what instrumentation will be required for the final installation. It is expected that the required instrumentation will be determined from the one meter dipole test for which a great deal of instrumentation will be provided. A list of instrumentation which will be used in the test is given below. Some subset of this selection will be standard instrumentation on each beam line magnet and on the proposed helium refrigeration system and transfer line.

Magnet

1. Six thermocouples - three at each end of the magnet.
2. A Vapor Pressure Thermometer (VPT) to measure the temperature of the liquid helium bath.
3. A mass flow meter to measure vent gas.
4. 9 voltage taps to measure the voltage across each coil.

Dewar

1. Liquid helium level.
2. Helium gas pressure.

Expansion Engine

1. 7 thermocouples at various points.
2. Piston stroke.
3. Cylinder pressure.
4. Two VPTs to measure inlet and outlet temperatures.

Lead Box

1. 18 thermocouples.

2. VPT to measure liquid helium temperature.
3. Liquid helium level.

Refrigerator

1. 8 thermocouples.
2. 4 VPTs.

Since there are a number of magnets needed for the transport system, the amount of instrumentation for each magnet will be kept small. It is currently planned to measure only the temperature of the liquid helium bath and the voltage drop across each magnet in order to diagnose quickly quench situations.

Control Consoles

A total of six control consoles and crates are planned for the High Intensity Laboratory. One console will be located in Service Building P3 and the other five in Service Building P4. Four of the five consoles in Service Building P4 will be for each of the operating experiments, whereas, the fifth will be for general Proton Department use.

*The relationship between the actual numbers of mistuned particles and the number of minimum ionizing particles passing through a loss monitor tube is not clear. If it is assumed that each minimum ionizing particle travels 10 cm in the tube and generates a primary ionization of 75 ion-electron pairs per centimeter, the collected charge from two tubes would be $2 \times 75 \times 10 \times 1.602 \times 10^{-19} = 2.4 \times 10^{-16}$ coulombs/minimum ionizing particles. Hence, to achieve 1 nc of charge, 4.2×10^6 minimum ionizing particles would have to pass through each tube.

Acknowledgments ████████

III. ACKNOWLEDGMENTS

Many people have contributed in many ways to the design of a project of this type and merit special thanks. I would especially like to give thanks to the management of the Laboratory, R. R. Wilson, E. Goldwasser, and J. Sanford for their support. Also, I would like to thank all the personnel of the Proton Department for their contributions, and to particularly thank J. Peoples, T. Murphy, P. Mazur, R. Rubinstein, L. Read, and my other physicist colleagues for much help. Other departments which have given much useful information and advice include Peter Gollon and the staff of Radiation Physics, and Dennis Theriot of the Neutrino Department. Finally, we would like to recognize Alice Lengvenis and Cindy Carra for many, many revisions of the various drafts of this report.

HIGH INTENSITY LABORATORY TRANSPORT* SYSTEM

Table Ia

Function	Distance from Target (Feet)	Component Type	Config/Fields [†] 500 /400 GeV-P/ GeV-S	Config/Fields [‡] 1,000 /800 GeV-P/GeV-S	Config/Fields [‡] 1,000 /1,000 GeV-P/GeV-S	
Proton Targeting Stage	Focussing Doublet	Q1	(1) 10.3 kg/in	(2) 10.3 kg/in	(2) 10.3 kg/in	
		Q2	(1) -10.7 kg/in	(2) -10.7 kg/in	(2) -10.7 kg/in	
	Horizontal Dogleg	TL/2	(1) -----	(1) -----	(1) -----	
	Horizontal Bend (10.97 m)	D1	(2) 33.0 kg	(3) 44.0 kg	(3) 44.0 kg	
	Vertical Trim	T2	(1) -----	(1) -----	(1) -----	
	Horizontal Pitching (7.31m) [§]	D2	(1) 44.0 kg	(2) 44.0 kg	(2) 44.0 kg	
Flux Collection Stage	Target Box Bend ⁺	D3	(1) 8.8 kg	(1) 17.6 kg	(1) 22.0 kg	
		Q3	(1) 10.5 kg/in	(2) 10.5 kg/in	(2) 13.1 kg/in	
	Focussing Triplet	Q4	(2) -8.2 kg/in	(3) -10.9 kg/in	(3) -13.6 kg/in	
	Dispersion	Q5	(1) 10.5 kg/in	(2) 10.5 kg/in	(2) 13.1 kg/in	
Stage	Dispersing Bend	D4	(2) 26.7 kg	(3) 35.7 kg	(3) 44.7 kg	
	Vertical Trim	T4	(1) -----	(1) -----	(1) -----	
FODO - Sextupole Correction Stage	Momentum Slit					
	Sextupole Correction No. 1	251.0	S1	(2) -14.2 kg/in ²	(4) -14.2 kg/in ²	(4) -14.1 kg/in ²
	FODO Quad	294.4	Q6	(1) -9.6 kg/in	(2) -9.6 kg/in	(2) -12.0 kg/in
	Vertical Trim	325.0	T5	(1) -----	(1) -----	(1) -----
	FODO Quad	351.1	Q7	(1) 9.6 kg/in	(2) 9.6 kg/in	(2) 12.0 kg/in
	Dispersion Cancellation	373.1	D5	(1) 25.8 kg	(2) 25.8 kg	(2) 32.3 kg
	FODO Quad	432.1	Q8	(2) -9.6 kg/in	(2) -9.6 kg/in	(2) -12.0 kg/in
	Dispersion Cancellation	454.1	D6	(2) 32.2 kg	(3) 42.9 kg	(3) 44.0 kg [#]
	FODO Quad	488.8	Q9	(1) 9.6 kg/in	(2) 9.6 kg/in	(2) 12.0 kg/in
	Dispersion Cancellation	510.8	D7	(1) 25.8 kg	(2) 25.8 kg	(2) 32.3 kg
	Sextupole Correction No. 2	534.4	S2	(2) -14.2 kg/in ²	(4) -14.2 kg/in ²	(4) -14.1 kg/in ²
Secondary Beam Targeting Stage	Focussing Triplet	564.9	Q10	(2) 8.7 kg/in	(3) 11.6 kg/in	(3) 14.5 kg/in
		603.2	Q11	(2) -9.7 kg/in	(3) -13.2 kg/in	(3) -14.6 kg/in [#]
	Vertical Trim	645.2	Q12	(2) 8.7 kg/in	(3) 11.6 kg/in	(3) 14.5 kg/in
	Horizontal Pitching [§]	678.2	D8	(1) -----	(1) -----	(1) -----
	F1 Focus	717.6		(2) -----	(2) -----	
TOTALS OF SUPERCONDUCTING MAGNETS			17 Quadrupoles 9 Dipoles 6 Trims 4 Sextupoles	26 Quadrupoles 14 Dipoles 6 Trims 8 Sextupoles	26 Quadrupoles 14 Dipoles 16 Trims 8 Sextupoles	

*Unless otherwise specified all fields are calculated based on the minimum magnet specifications in Table II.

+Conventional B-2 magnet.

‡Pion transport tune for F1 focus.

#Field limit reached for dipole and quadrupole. Precise scaled up tune not possible at 1,000 GeV.

§Needed eventually for experiments are the four horizontal pitching magnets.

TABLE Ib. CONVENTIONAL 300-GeV TRANSPORT SYSTEM

Function	Component Type	Fields*		Power Consumption	KVA*
		500/300 GeV	p/GeV S		
Proton Targeting Stage	Focussing Doublet	Q1	2 5.15 kg/in	98	
		Q2	2 -5.35 kg/in	102	
	Horizontal Dogleg	T1/2	1 -----	6	
	Horizontal Bend (10.97 mr)	D1	4 16.5 kg	306	
	Vertical Trim	T2	1 -----	6	
	Horizontal Pitching (7.31 mr)	D2	2 16.5 kg	220	
Flux Collection Dispersion Stage	Target Box Bend**	D3	1 6.6 kg	75	
		Q3	2 3.9 kg/in	74	
	Focussing Triplet	Q4	3 -4.1 kg/in	155	
		Q5	2 3.9 kg/in	74	
	Dispersing Bend	D4	3 13.4 kg	178	
	Vertical Trim				
FODO - Sextupole Correction Stage	Sextupole Correction #1	S1	4 5.3 kg/in ²	490	
	FODO Quad	Q6	2 -3.6 kg/in	68	
	Vertical Trim	T5	1 -----	6	
	FODO Quad	Q7	2 3.6 kg/in	68	
	Dispersion Cancellation	D5	2 9.7 kg	65	
	FODO Quad	Q8	2 -3.6 kg/in	68	
	Dispersion Cancellation	D6	3 16.2 kg	215	
	FODO Quad	Q9	2 3.6 kg/in	137	
	Dispersion Cancellation	D7	2 9.7 kg	65	
	Sextupole Correction	S2	4 -5.3 kg/in ²	490	
Focussing Triplet		Q10	3 4.3 kg/in	175	
		Q11	3 4.9 kg/in	185	
		Q12	3 4.3 kg/in	162	
	Vertical Trim	T6	1 -----	6	
	Horizontal Pitching	D8	1 -----	100	

*The quadrupoles in this conventional arrangement could be 3Q120 or 4Q120 models.
 The dipoles could be either EPB dipoles or 6-3-120 benders.
 The sextupoles would have to be developed.

*KVA TOTAL 3594

High Intensity Laboratory Minimum Magnet Specifications

Table II

	<u>Max Field *</u> <u>at Pole Tip</u>	<u>Gradient</u>	<u>Field</u> <u>Length</u>	<u>Total**</u> <u>Length</u>	<u>Good Field</u> <u>Aperture</u>	<u>Current</u>
Dipole	44 kg	-	108"	120"	3"v x 5"h	***200 a
Quadrupole	44 kg	14.6 kg/in	108"	120"	6" circular	200 a
Sextupole	44 kg	19.6 kg/in ²	80"	90"	3" circular	200 a
Trims	44 kg	-	38"	48"	5" circular	200 a

* Field needed for 1000 GeV operation.

** Total length includes cryogenics plumbing and possible valve.

*** A 2400 amp magnet is being fabricated by the Research Division, but because of ease of setup and minimization of heat load, 200a is preferred.

TABLE III

HIGH INTENSITY TRANSPORT

FOCAL PROPERTIES*

The sizes quoted here and in the figures are rms half widths based on TURTLE histograms.

Focal Point	σ_X	σ_Y	$\sigma_X l$	$\sigma_Y l$	Transmission
F1 (717.6')					
Sextupoles Off	.210 cm	.466 cm	.685 mrad	.518 mrad	99%
F1 (717.6')	.226 cm	.195 cm	.832 mrad	.540 mrad	71%
F4 (799.2')					
Sextupoles Off	4.397 cm	1.371 cm	.296 mrad	.445 mrad	-
F4 (799.2')					
Sextupoles Off	13.76 cm	3.181 cm	.299 mrad	.055 mrad	-

*All focussing characteristics are calculated assuming the proton targeting characteristics given in the text. The quoted numbers are the results of a complete ray tracing by TURTLE for a 5% momentum bite and a .75 mrad production cone for the F1 results. The F4 results are for the same production cone and momentum bite but with the beam tuned for maximum parallelism in σ_Y . The quoted numbers are the result of a transport calculation so no transmissions are given.

TABLE IV

PION BEAM - ESTIMATED POWER REQUIREMENTS

TARGET SERVICE BUILDING

<u>QUANTITY</u>	<u>DEVICE</u>	<u>TOTAL KVA</u>
1	Transrex 500 Power Supply	715
10	Cryogenic Power Supplies	400
2	Chillers	308
1	Compressor	275
4	Air Coolers	40
2	Glycol Pumps	20
1	Expansion Engine	10
	Miscellaneous Heating, Cooling, and Distribution	<u>300</u>
	<u>Total</u>	<u>2068</u>

EXPERIMENTAL HALL

2	Transrex 500 Power Supplies	1430
14	Cryogenic Power Supplies	560
1	Compressor	275
2	Pumps	80
2	Towers	40
	HVAC for Building	60
	Miscellaneous Heat, Light, and Distribution	<u>600</u>
	<u>Total</u>	<u>3045</u>

Table V. Instrumentation Requirements

SWIC	CHAMBER RESOLUTION	APPROXIMATE DISTANCE FROM TARGET	LOCATION	TRANSPORT			CALCULATIONS (F1 Focus)		
				X - PROFILE			Y - PROFILE		
				FULL WIDTH	FWHM	*Nipk	FULL WIDTH	FWHM	*Nipk
#1	1 mm	- 41 ft							
#2	.5 mm	-1 ft							
#3	2 mm	228 ft	234 ft	540 mm	28 mm	.075I	13 mm	4 mm	.376I
#4	2 mm	269 ft	274 ft	>40 mm	36 mm	.060I	31 mm	4 mm	.294I
#5	2 mm	331 ft	315 ft	108 mm	20 mm	.057I	100 mm	8 mm	.139I
#6	2 mm	423 ft	432 ft	14 mm	20 mm	.074I	160 mm	16 mm	.054I
#7	2 mm	513 ft	X 489 ft Y 549 ft	44 mm	20 mm	.078I	30 mm	6 mm	.175I
#8	1 mm	545 ft	549 ft	18 mm	3 mm	.185I	30 mm	6 mm	.096I
#9	1 mm	717 ft	717 ft	14 mm	2 mm	.239I	20 mm	2 mm	.193I

*Nipk = Fraction of full intensity on peak wire based on Resolution in Col. 1.

TITLE - SCHEDULE

TABLE - VI

	PROTON MECHANICAL, CYRO- ELECTRICAL AND CYRO-MKIB INSTRUMENTATION	ARCHITECTURAL WORK	SUPERCONDUCTING* MAGNETS	MAGNET INSTALLATION SEQUENCE	GOALS
Jan., 76		Manholes/Conduits for			
Feb., 76		Upstream Area Complete	+ Quad Prototype		
		Bid Package Phase I ready	(2') design begins		
March, 76	+ Prototype Transfer	Design Package Phase II ready.	+ One meter prototype finished		
	Line Finished	Civil Design Mech., Elec.,	+ Quad design finished		
April 76		Phase II Design Finished	+ Phase I & II	+ Testing 1 meter prototype	
May, 76	+ Mechanical Design Finished				
June, 76	on Target Box/transporter	+ Construction			
		Phase II begins			
July, 76	+ Mechanical Design Momentum		+ Sextupole design finished		
	Slit/Finisher				
Aug., 76	Mechanical Design Upstream				
	Dump Finished				
Sept., 76	+ Mechanical Design Upstream	+ Civil Work			
	Collimator	Complete on			
Oct. 76	+ Mechanical Design Magnet	Tunnel			
Nov., 76	Transporter done	+ Substations			
		Installed.			
Dec., 76	+ Transfer line complete in	+ Civil Work	+ 3 meter dipoles finished (2)		
	Downstream P-West	complete on			
Jan., 77		enclosures			
Feb., 77			+ Prototype Quad (2')		
			finished & tested.		
March, 77		+ Civil Work			
		complete on			
April, 77		service bldg.	+ Civil Work		
			complete on		
May, 77	Rework of P-Westbeam Dump	exp bldg.	Prototype Quad (3M) finished		
	& Collimator installation		& tested.		
	complete			Install 3 meter magnets	Bring Proton Beam to
				as first stage safety	P-West Dump
				bend & tes.	
June, 77	+ Installation of Cryogenics	+ Steel erected			
	finished in tunnels	to beam pipe.	+ Next 4 dipoles tested &		
		installed	ready.		
		from P-2			
July, 77			+ First 2 Quads ready.	+ Install Quads in downstream	
				P-WZ.	
Aug., 77	Installation of Target Box done	Mechanical			
	Interlocks complete the entire	finished	+ Prototype Sextupole done.		Target Proton Beam Pion Lab
	area				
Sept., 77	+ Installation of Momentum slit				
	Magnet Transporter complete		+ Next 4 Quads ready.	+ Install Quads (4)	
				Install 2 dipoles behind	
				target box.	
Oct., 77	+ Refrigerator installation				
	Upstream service bldg. complete				
Nov., 77			+ Next 4 Quads. Next 4 dipoles.	+ Install FODO section &	Focus Secondary Beam on
				dipoles	Momentum slit.
Dec., 77	+ Refrigerator installation				
	downstream service bldg. complete				
Jan., 78					Transport Secondary Beam
			+ Next 6 Quads.		through FODO section.
Feb., 78	+ Instrumentation installation				
	complete				
March, 78	+ First Exp. installation complete			+ Install Targeting Section.	Target Secondary Beam on Fl.
April, 78			+ First 4 Sextupoles available.	+ Install Sextupoles.	Now CUV Secondary Transport
					complete.
May, 78					
June, 78					

TABLE VIIa

PLANT COST ESTIMATE SUMMARY

	<u>PHASE I</u>	<u>PHASE II</u>	<u>TOTAL</u>
Architectural & Civil	954,000	386,000	1,340,000
Beam Pipe (Steel Shielding by Fermilab)	-0-	22,000	22,000
Electrical	254,000	129,000	383,000
Mechanical	<u>68,000</u>	<u>39,000</u>	<u>107,000</u>
TOTAL	1,276,000	576,000	1,852,000

TABLE VIIB

EQUIPMENT ESTIMATE (1000 GeV Configuration)

I.	Shielding Steel (Outside PW-3) 1245 tons	230K
II.	P-West Beam Dump Modification	
	a. Dump Modification	20K
	b. Collimator	10K
III.	Proton Targeting/Safety Switch	
	a. Superconducting Quads (4)	160K
	b. Superconducting Dipoles (3)	120K
	c. Superconducting Power Supplies (3)	27K
	d. Instrumentation/Controls/Cabling	10K
	e. Transfer Line	20K
	f. Miscellaneous (Stands, Interlocks, etc.)	<u>33K</u>
		370K
IV.	Proton Target Box	
	a. Targeting Dipoles (2)	80K
	b. Chiller	50K
	c. Target Box Steel (871 tons)	110K
	d. Be Target Assembly	10K
	e. B2 Assembly	20K
	f. Dump/Collimator Assembly	50K
	g. Target Box Fabrication/Assembly	70K
	h. Instrumentation/Controls/Cabling	10K
	i. Electrical Hookup	20K
	j. Miscellaneous	<u>20K</u>
		440K
V.	Secondary Beam Transport (1000 GeV Superconducting) to F1 Focus	
	a. Superconducting Quads (22)	880K
	b. Superconducting Dipoles (9)	360K
	c. Superconducting Sextupoles (8)	240K
	d. Power Supplies (14)	130K
	e. Momentum Slit (Including 363 tons FE)	50K
	f. Refrigeration System (Satellite Refrigerators - 2)	440K
	g. Transfer Line	100K
	h. Vacuum Pipe/Pumps	30K
	i. Instrumentation/Controls/Cabling	20K
	j. Targeting Dipoles	<u>80K</u>
		2330K

TABLE VIIb (Continued)

VI. Experimental Area

a. π , p, e^{\pm} Targets/Targeting Systems	90K
b. Controls/Instrumentation	40K
c. Shielding*	100K
d. Set-up of Counting Areas/PS Facility	100K
e. Beam Dump	50K
f. Miscellaneous	<u>40K</u>
	420K
Total	<u>3820K</u>

*Only part of shielding is costed. We assume \sim 200K of PPA concrete shielding is available.

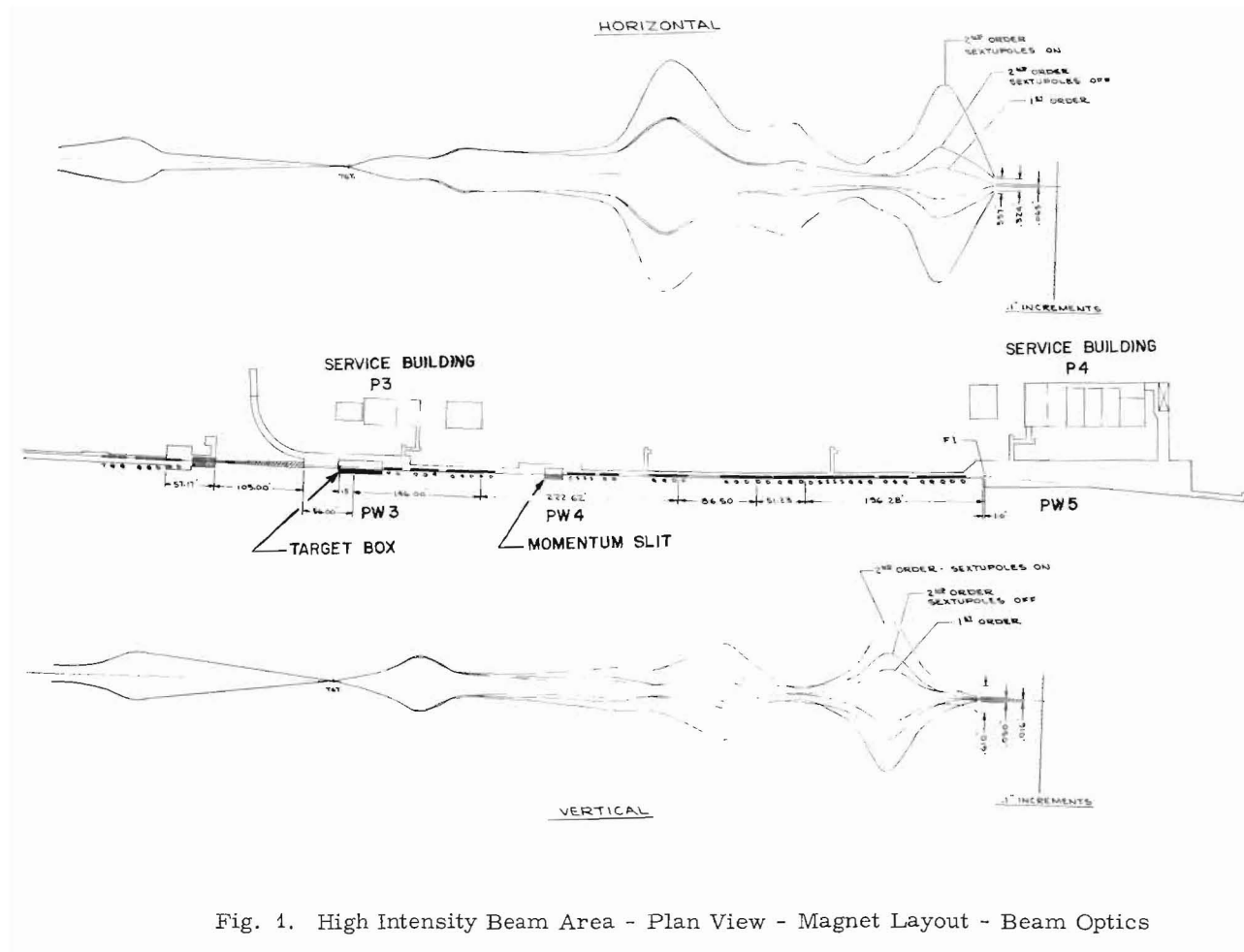


Fig. 1. High Intensity Beam Area - Plan View - Magnet Layout - Beam Optics

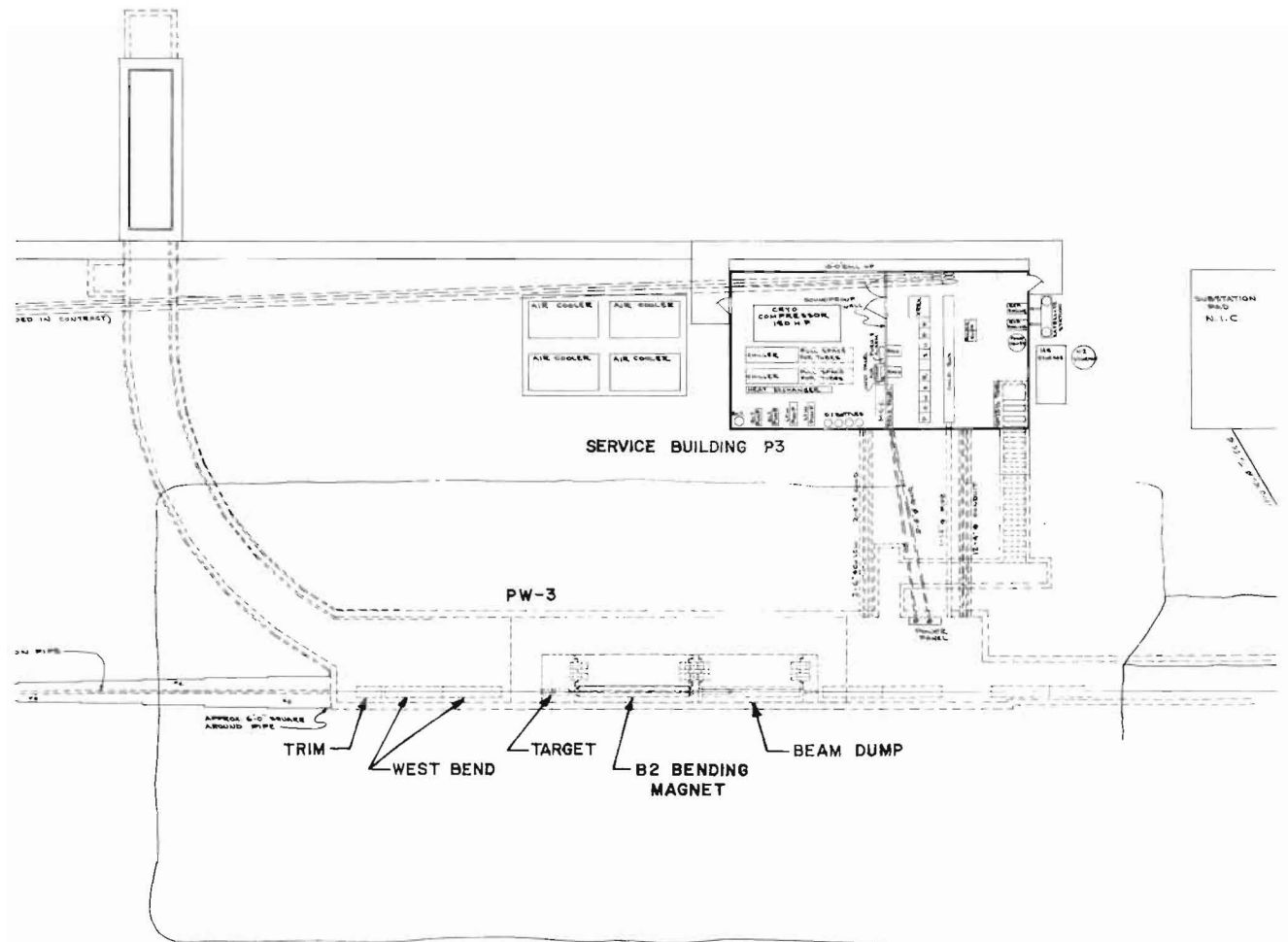


Fig. 2(a). Proton Targeting Station (PW-3)

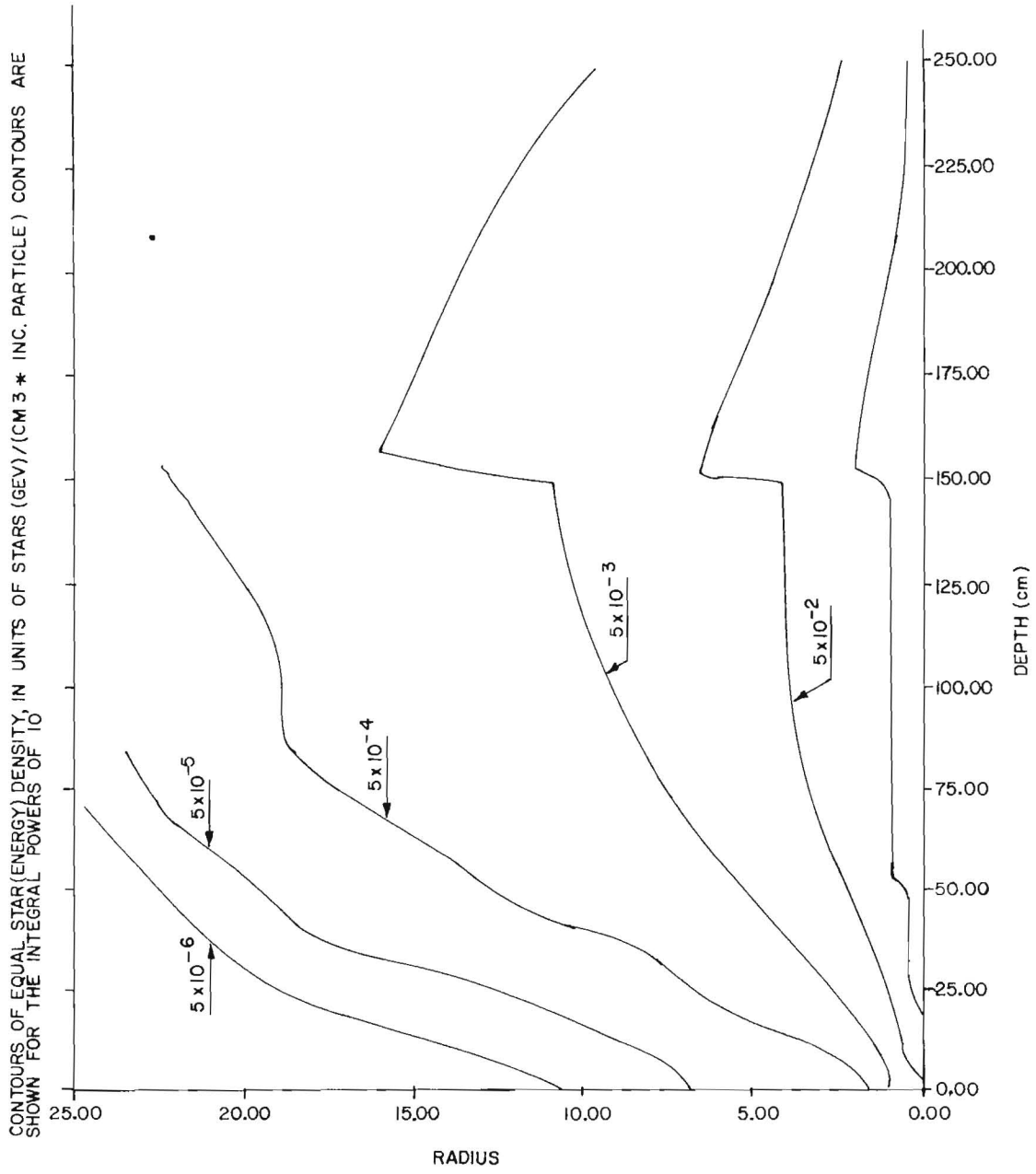
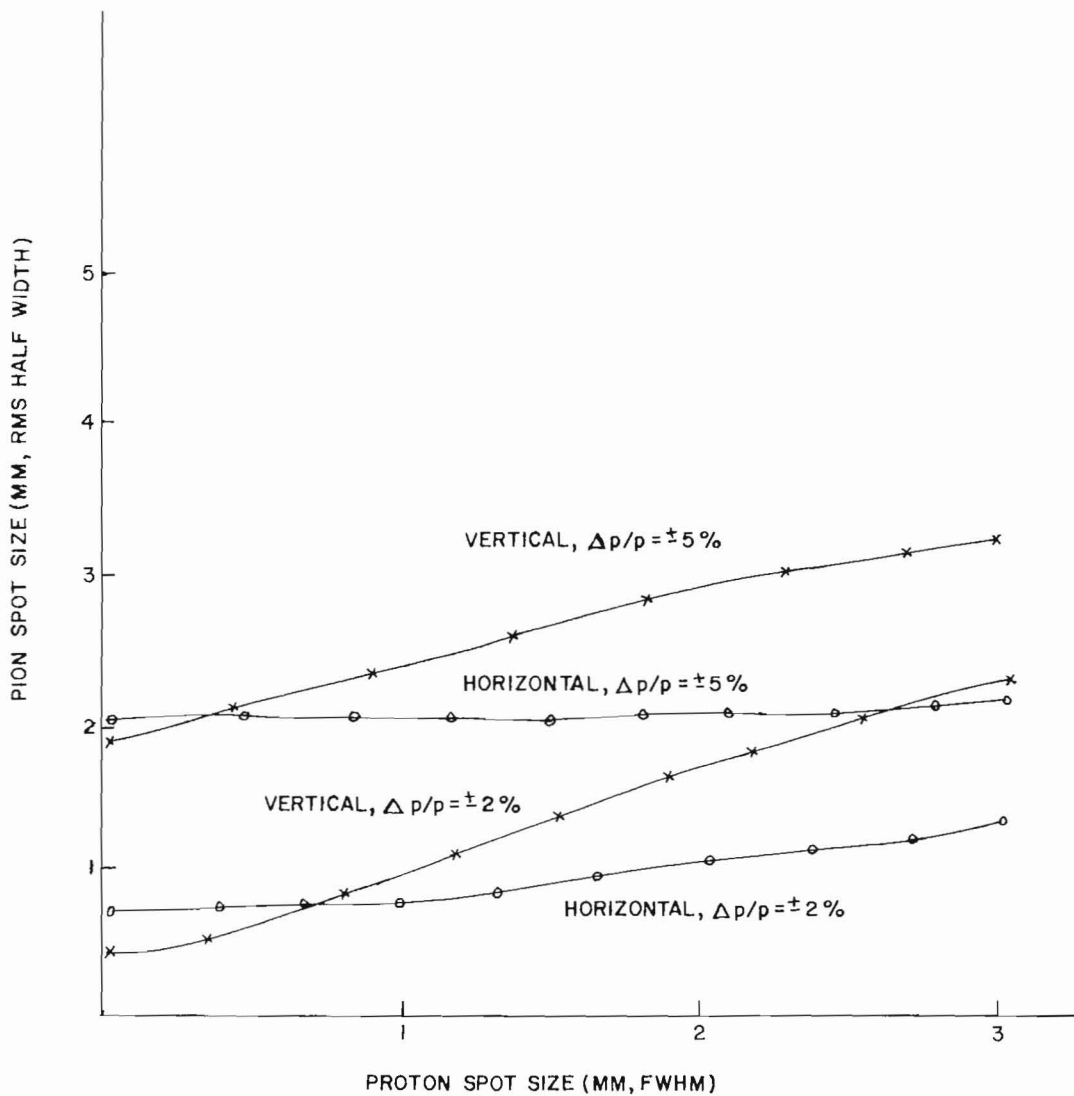


Fig. 2(c). Energy Deposition Curves - Proton Beam Dump

PION BEAM SPOT SIZE
AT FI Vs PROTON BEAM
SPOT SIZE



NOTE:

$\sigma_{x\pi}$ AND $\sigma_{y\pi}$ ARE FUNCTIONS ONLY OF σ_{xp} OR σ_{yp} .
THEY ARE NOT CROSS COUPLED

Fig. 3(a). Secondary Beam Spot Size (rms half-width) vs. Proton Target Spot Size (FWHM)

SECONDARY BEAM SPOT
SIZE AT F1 Vs ACCEPTANCE ANGLE

$$\left(\frac{\Delta p}{p} = \pm 5\% \right)$$

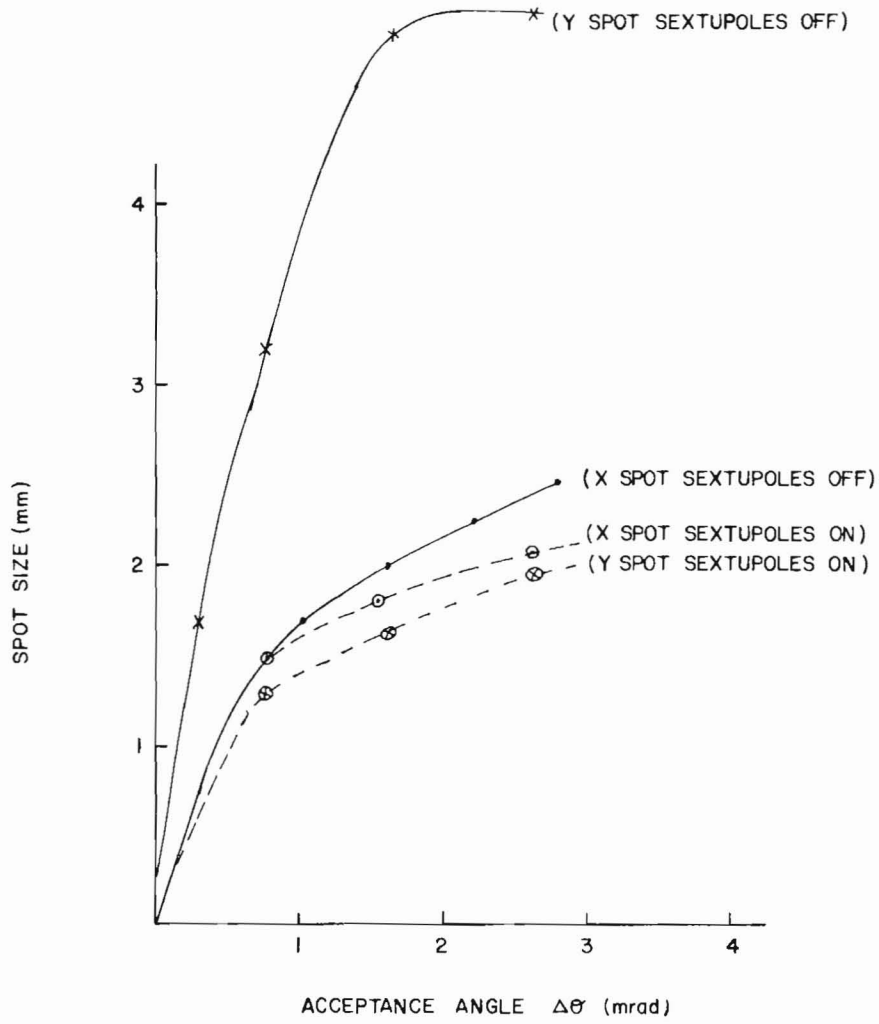


Fig. 3(b). Secondary Beam Spot vs. Angular Acceptance (F1).

SECONDARY BEAM SPOT
SIZE Vs MOMENTUM BITE
AT F1 FOCUS
($\pm .75$ mrad CONE)

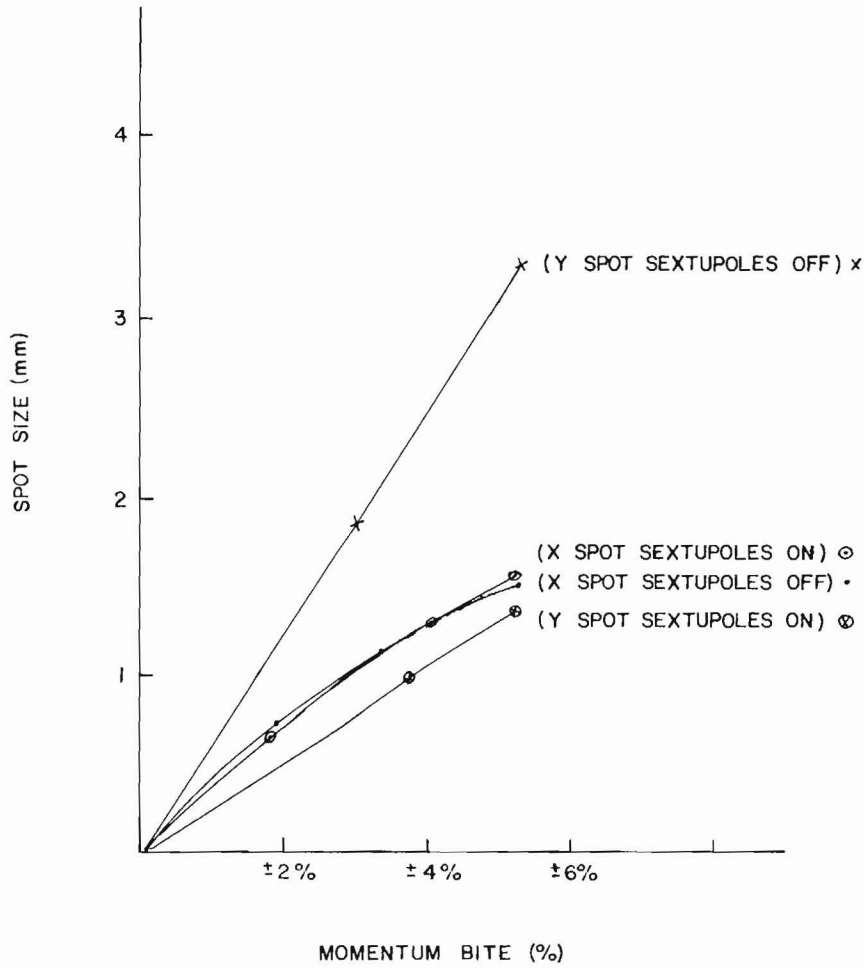


Fig. 3(c). Secondary Beam Spot Size vs. Momentum Bite (F1)

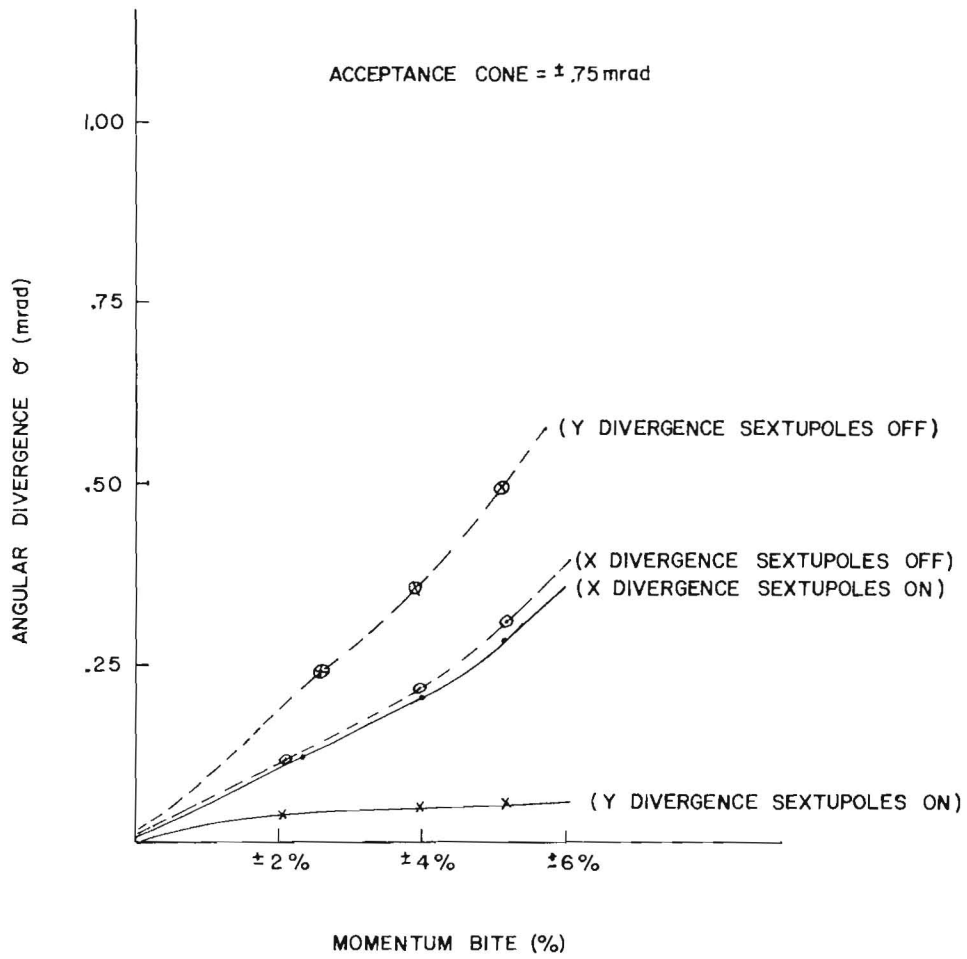


Fig. 3(d). Secondary Beam Parallelism vs. Momentum Bite (F4)

MOMENTUM BITE = $\pm 5\%$

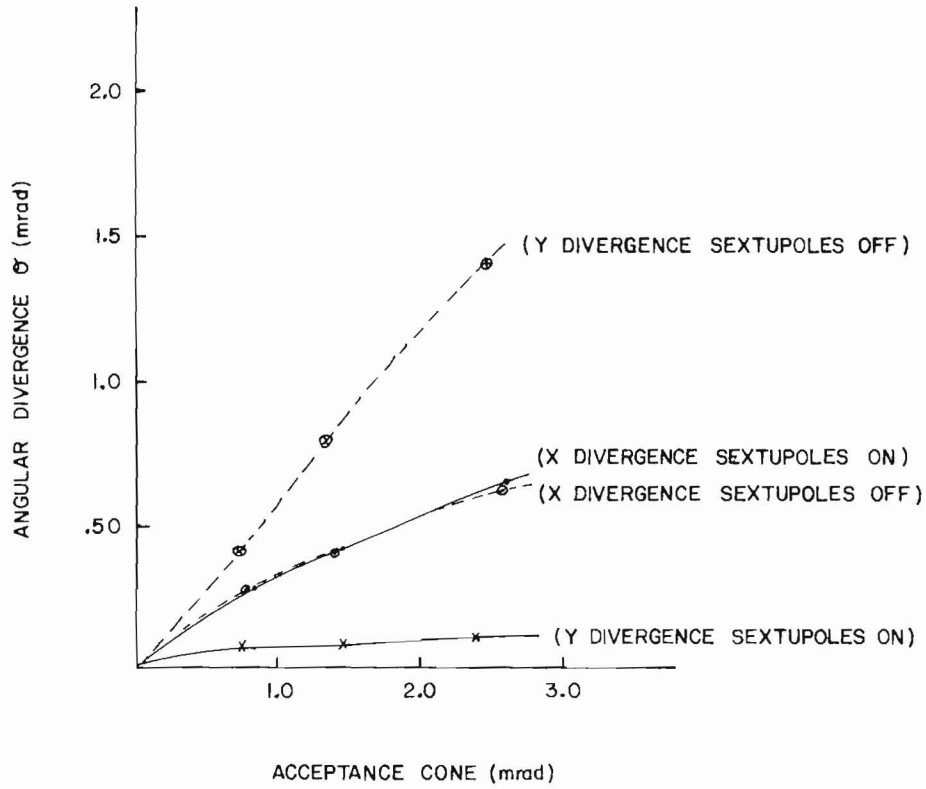


Fig. 3(e). Secondary Beam Parallelism vs. Angular Acceptance (F4)

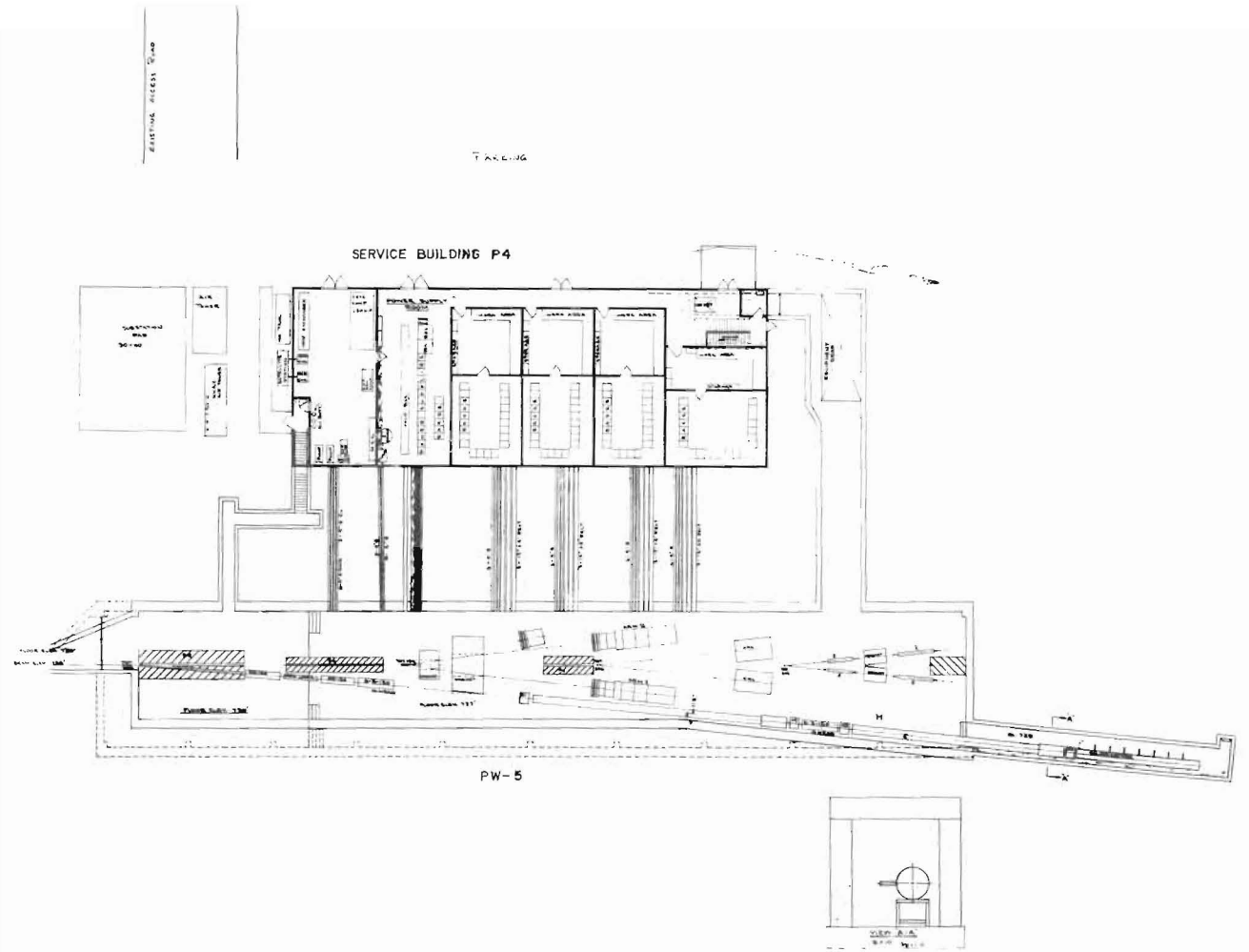


Fig. 4. Experimental Area and Service Building (PW-5)

YIELD CURVES vs ACCEPTANCE ANGLE WANG FITS.

$X = P_{\pi} / P_{\text{incident}} = .25$

LABELS ON CURVES ARE (PARTICLE, $\pm \Delta p/p$)

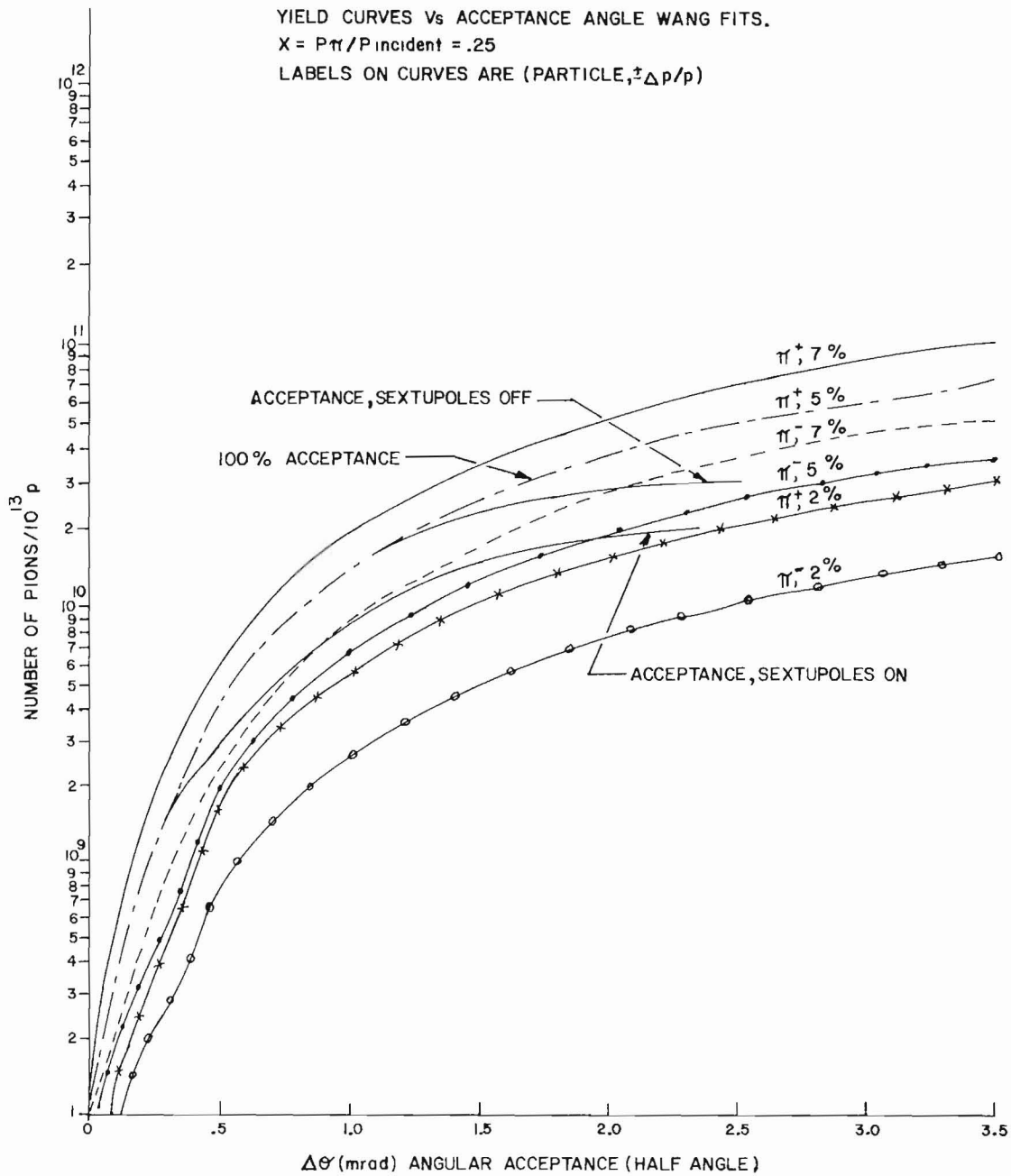


Fig. 5(a). π^\pm Yields vs. Angular Acceptance 400 GeV

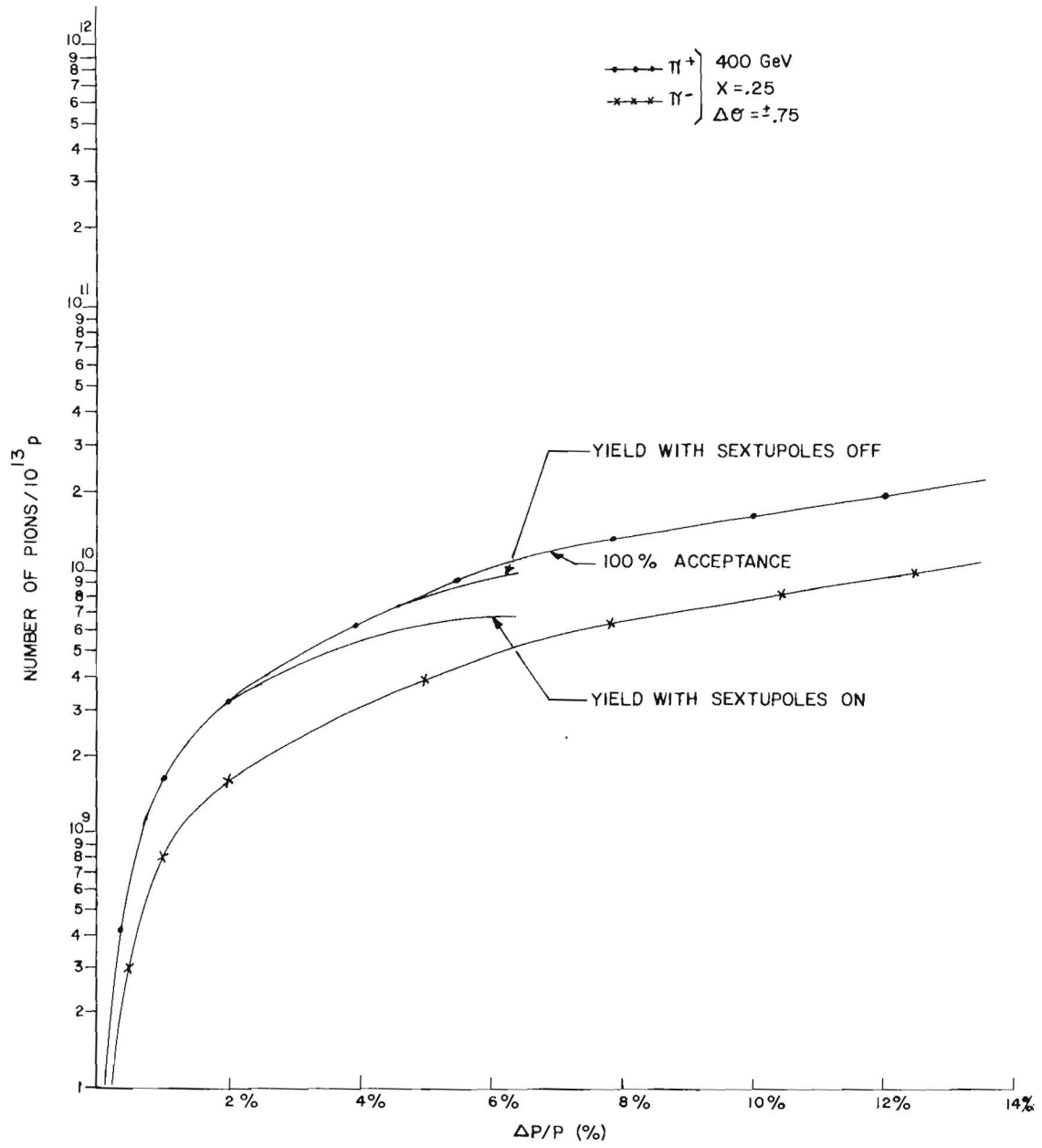


Fig. 5(b). π^\pm Yields vs. Momentum Bite (Wang Fits)

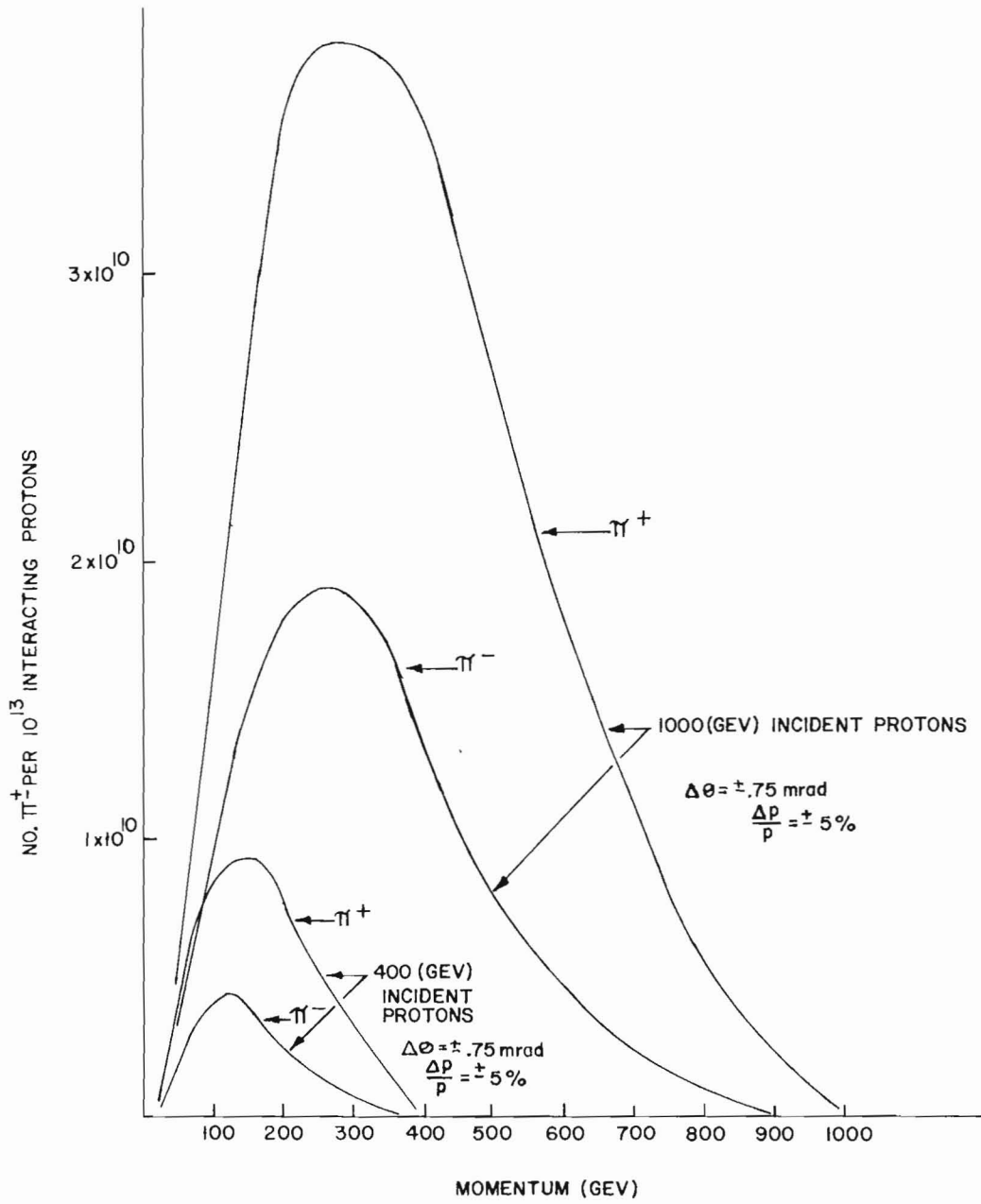


Fig. 5(c). π^\pm Yields vs. Energy of the Secondary Beam

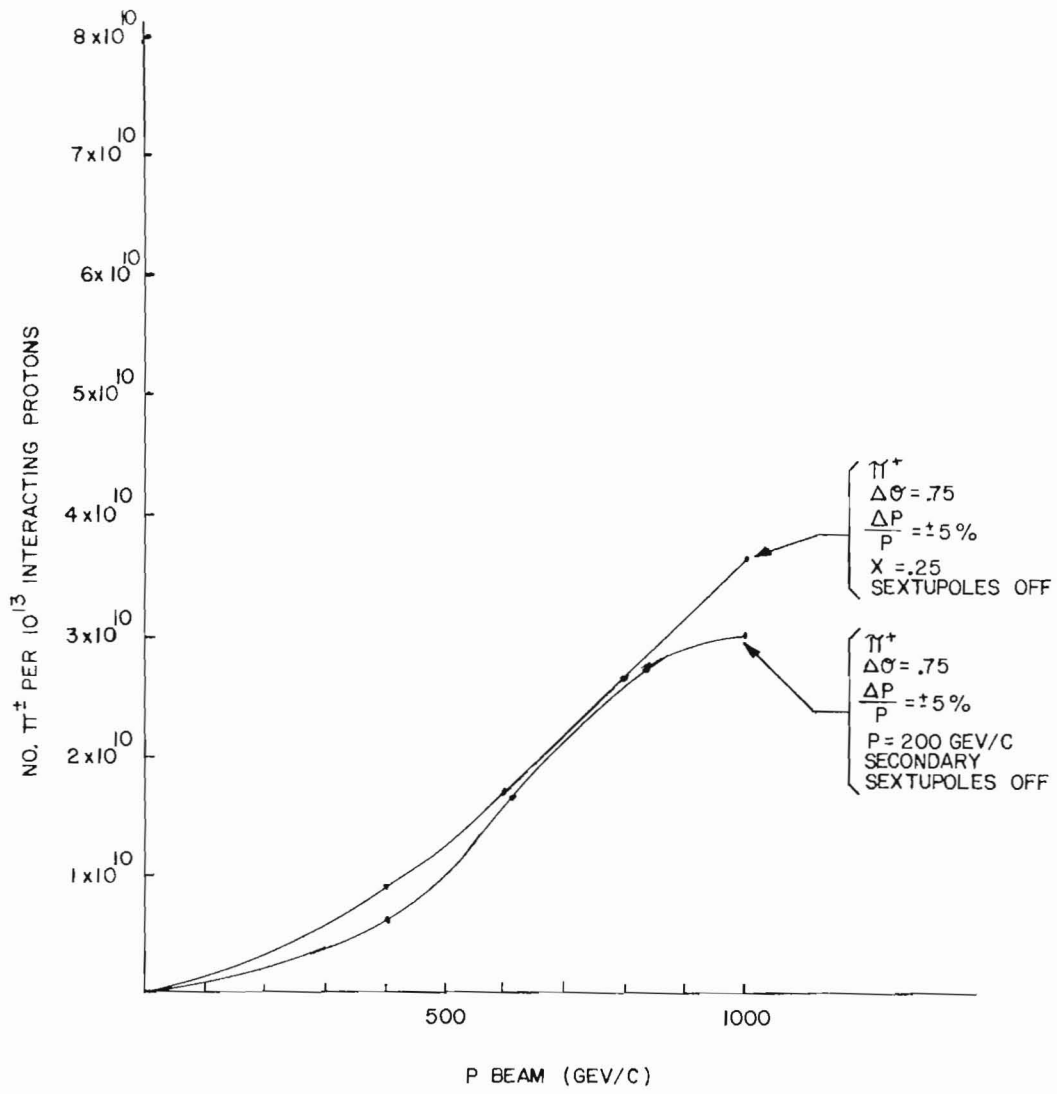


Fig. 5(d). π^\pm Yields vs. Energy of the Proton Beam

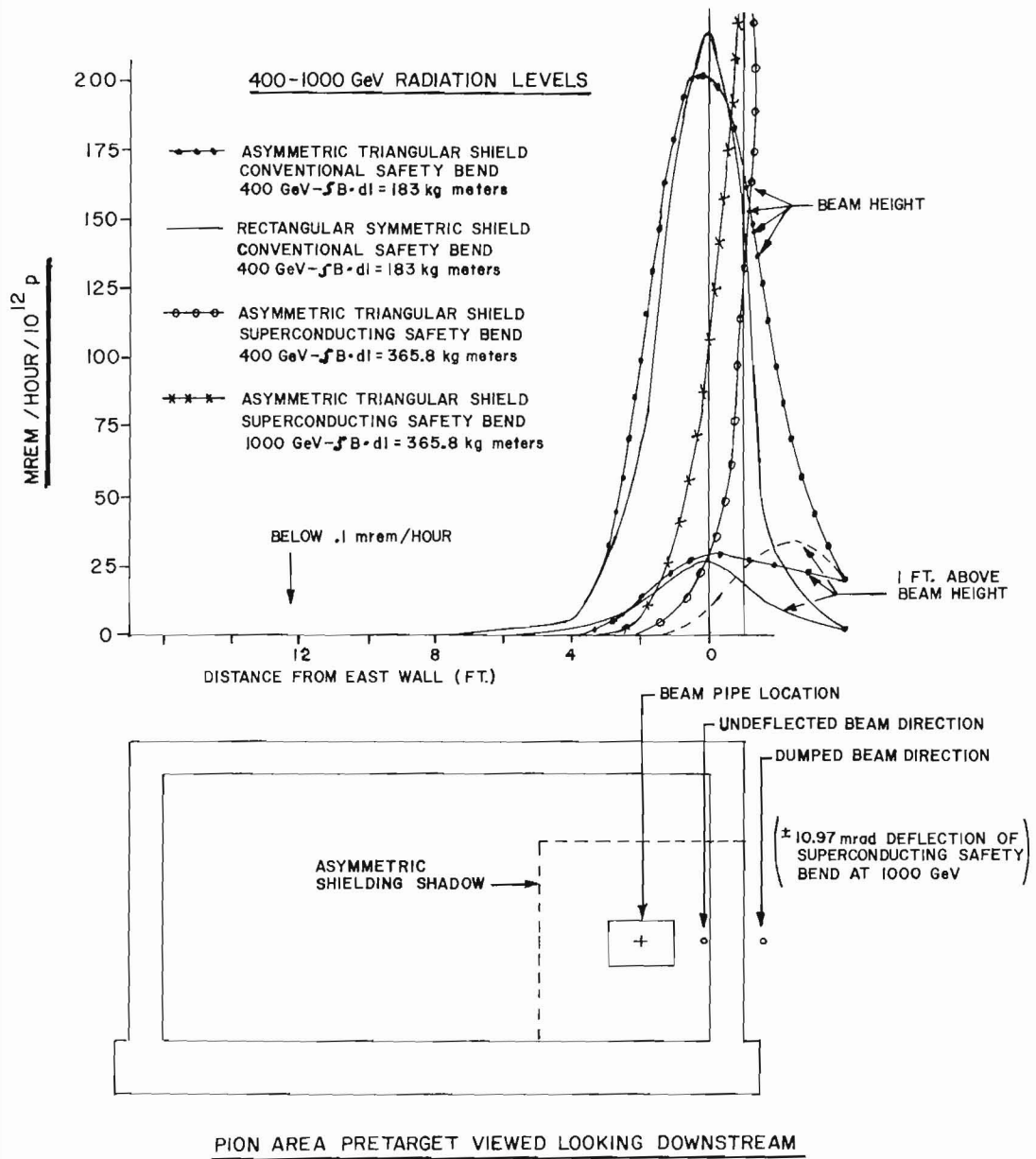


Fig. 6(a). Radiation Levels in PW-3 During Operation of PW-1 Area

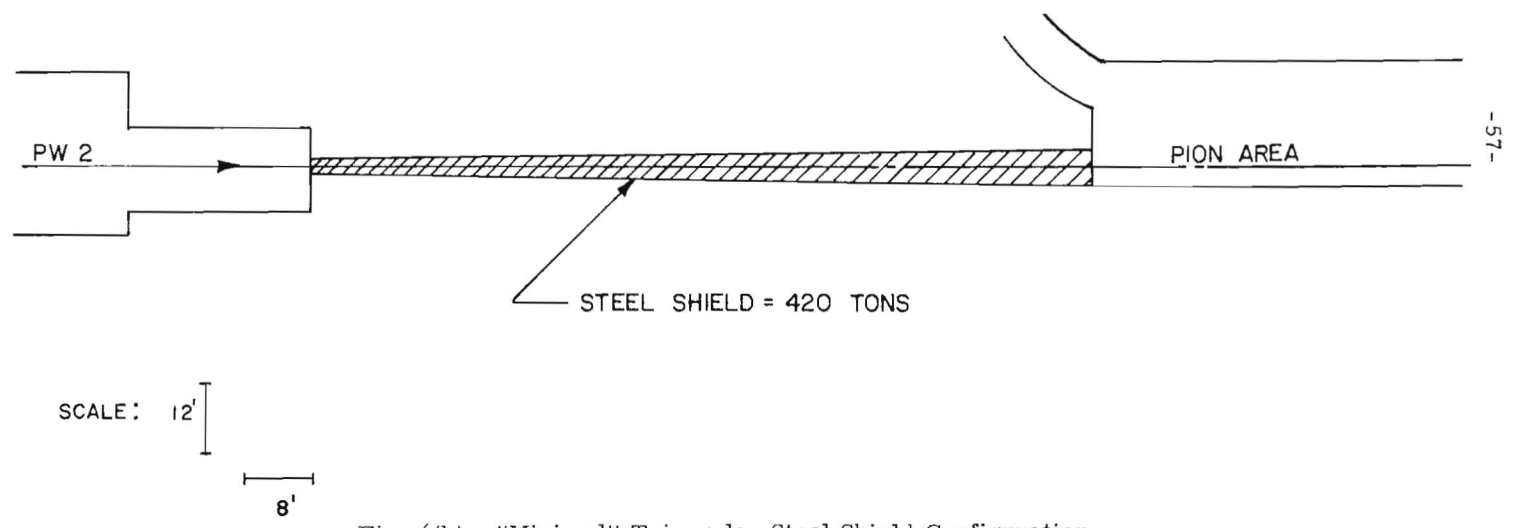


Fig. 6(b). "Minimal" Triangular Steel Shield Configuration

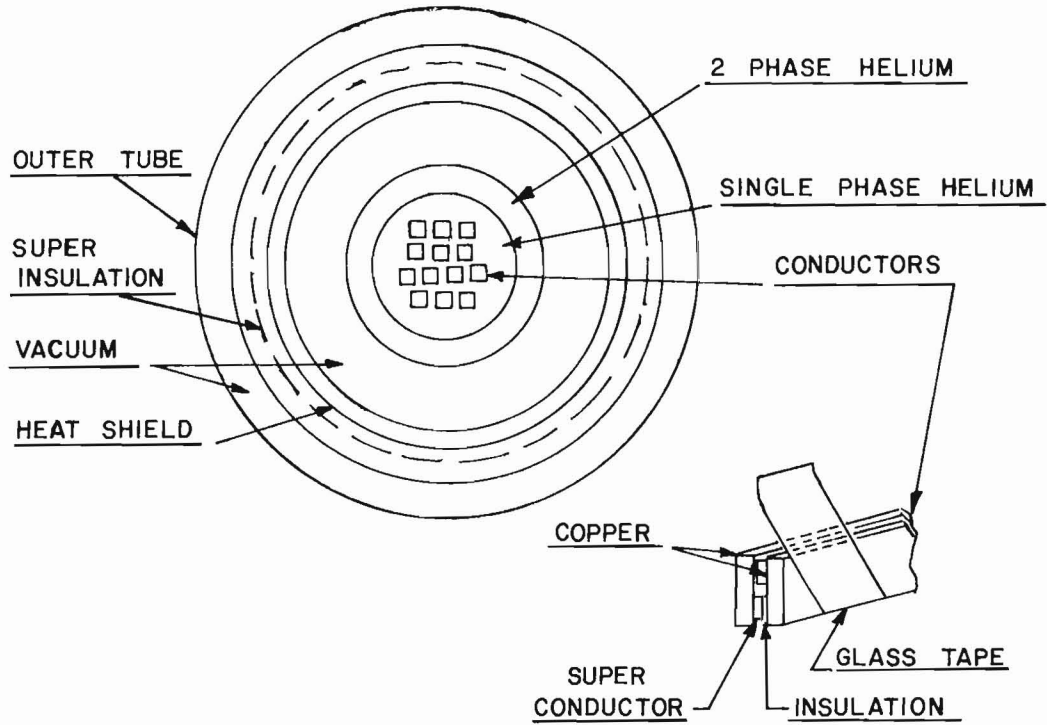


Fig. 7. 3000 Amp Transfer Line and Conductor

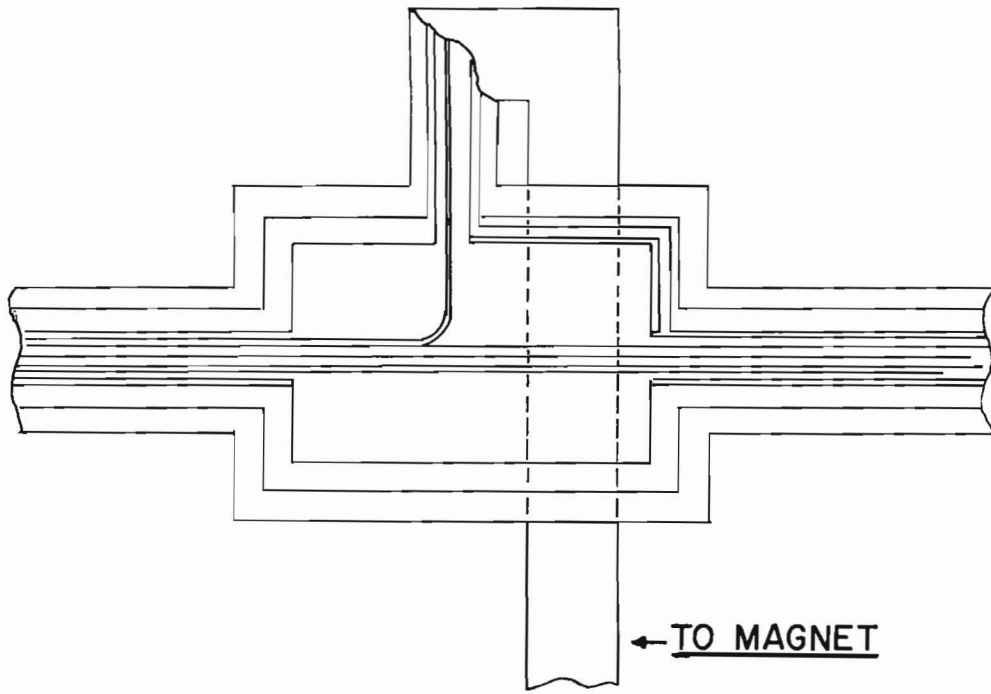


Fig. 8. 3000 Amp Transfer Box

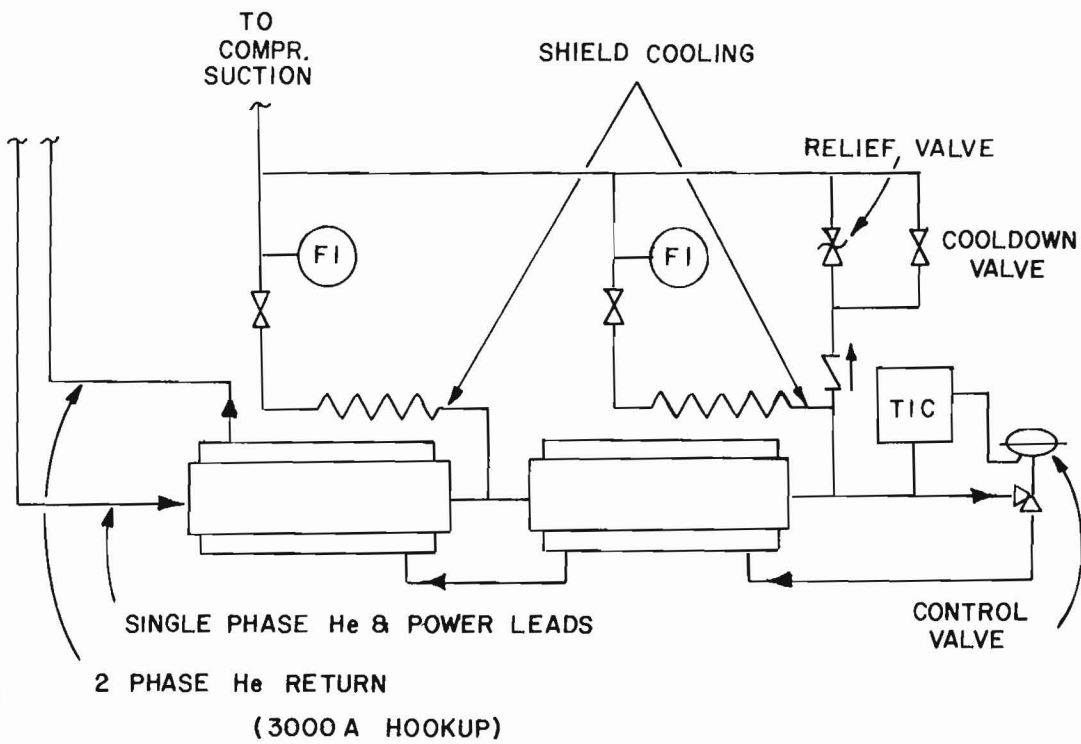


Fig. 9. Helium Circuit Drawing at Magnet

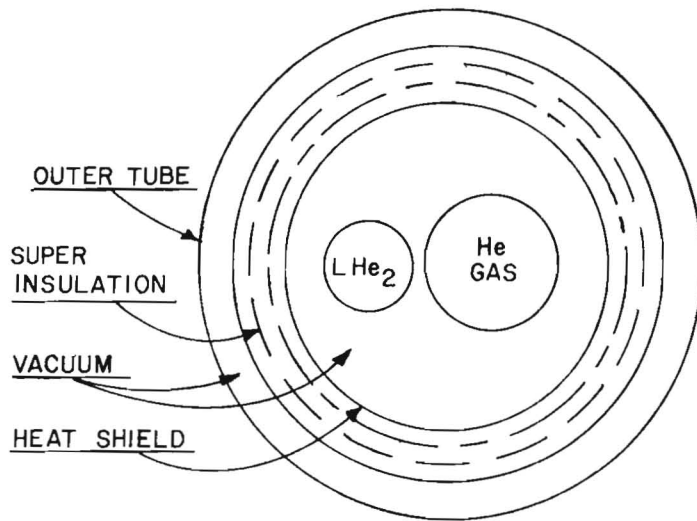


Fig. 10. 200 Amp Transfer Line

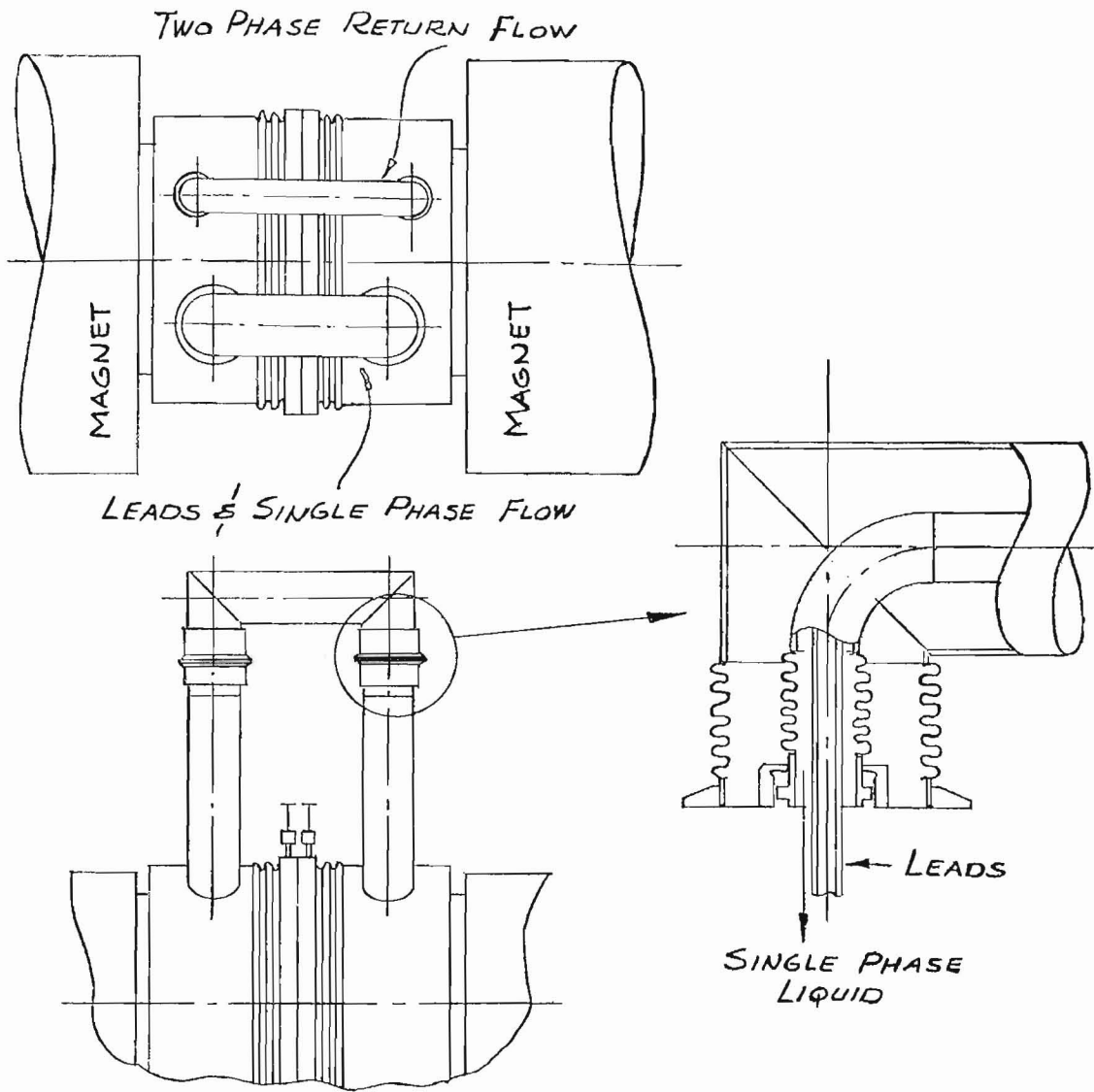


Fig. 11. Inter-Magnet Helium Plumbing

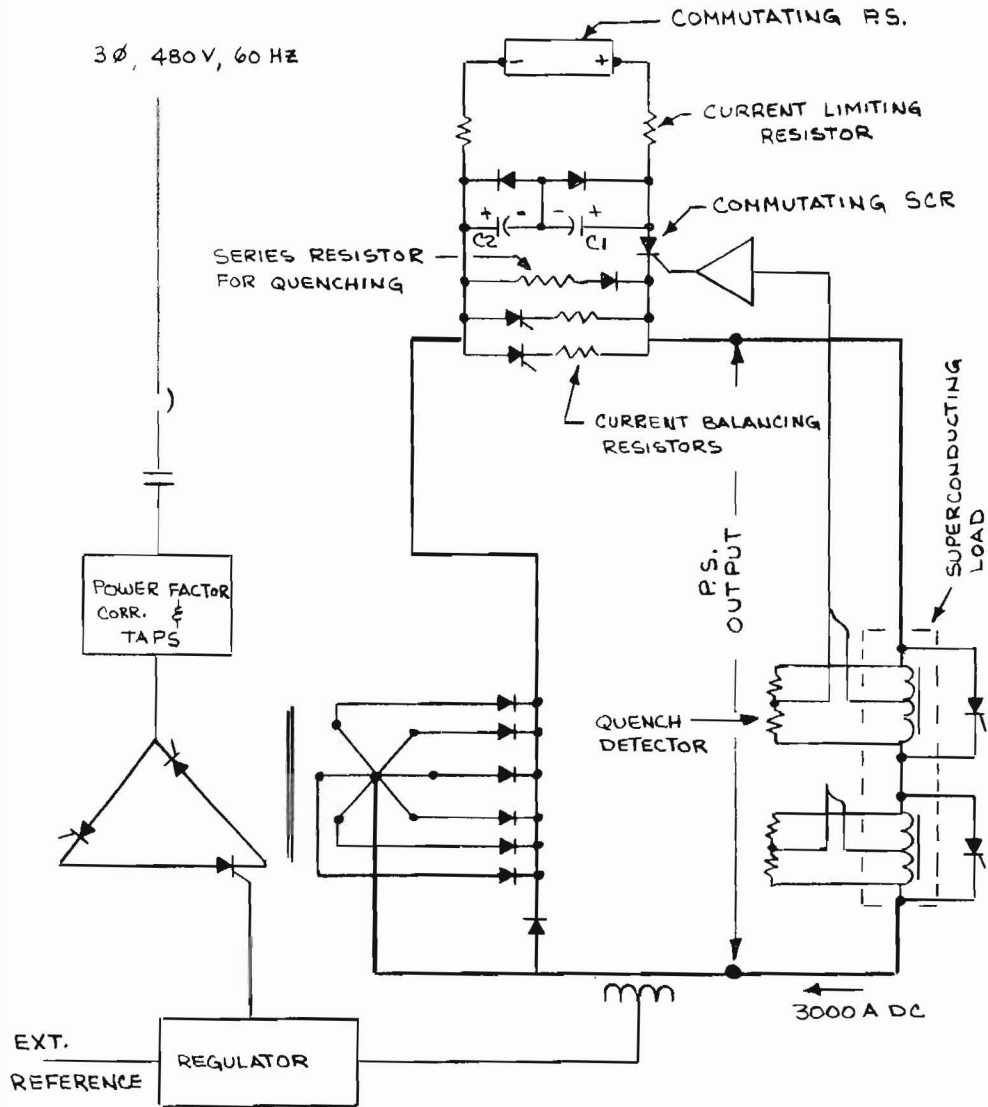


Fig. 12. Superconducting Magnet Power Supply with Built In Quenching Circuit

POWER FLOW DIAGRAM

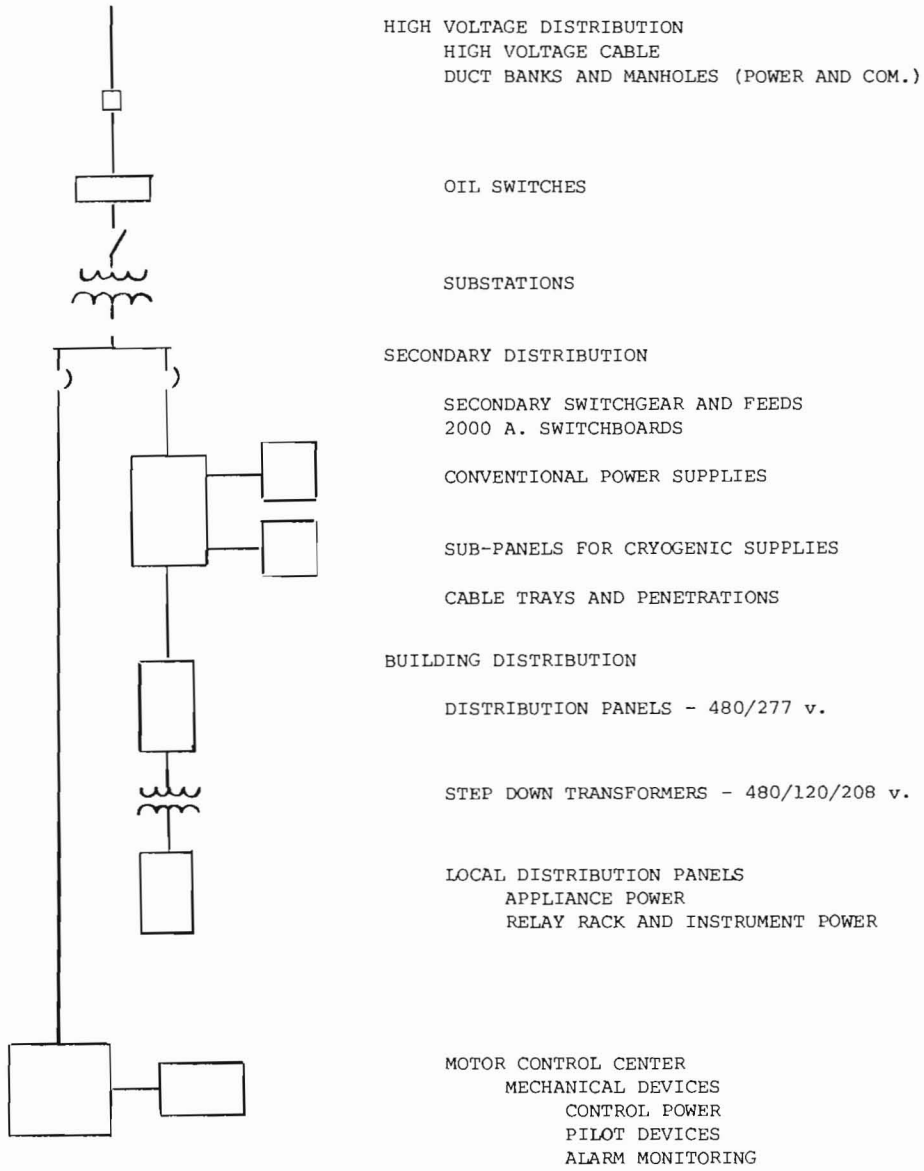


Fig. 13. Electrical Power Flow Diagram

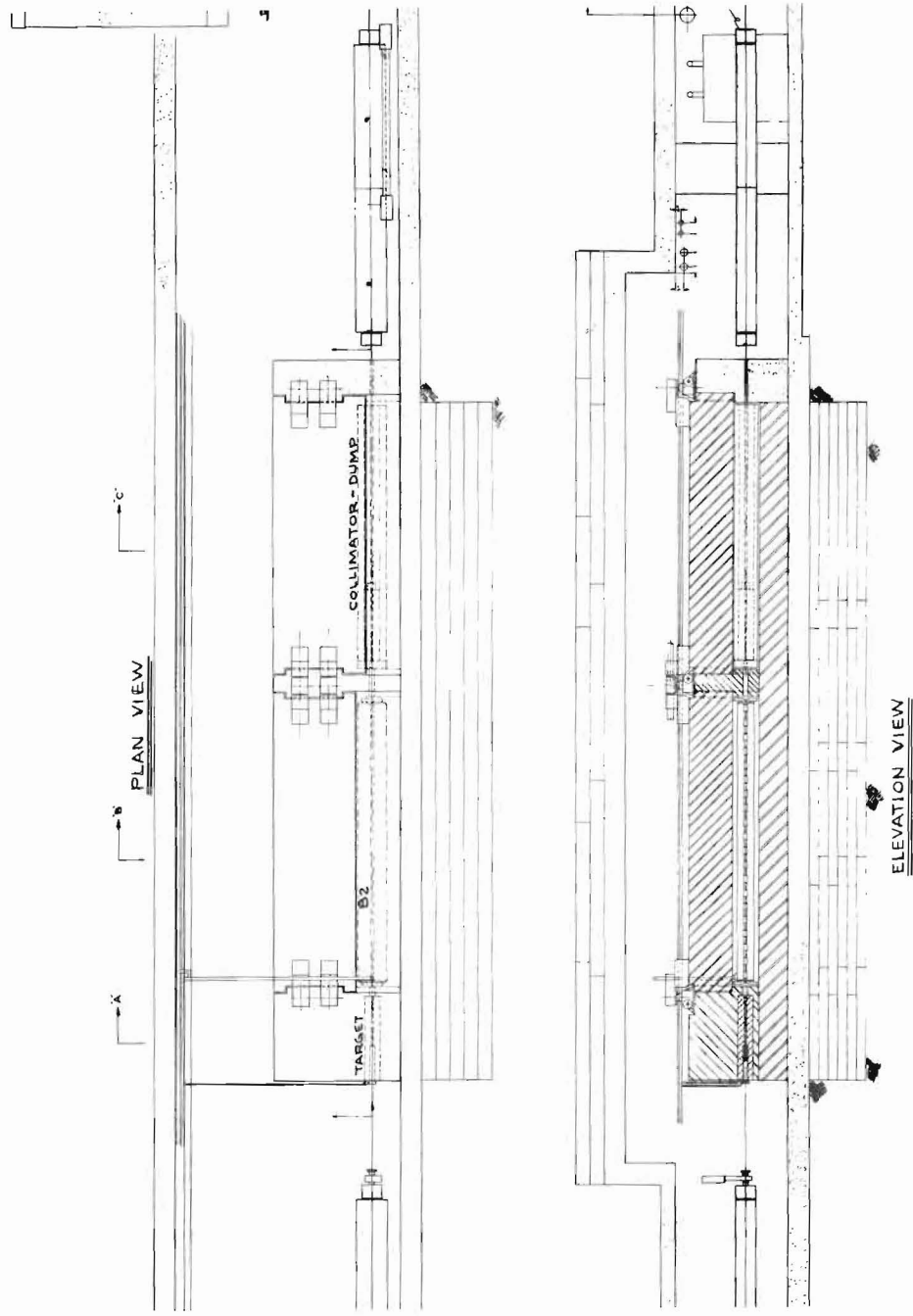


Fig. 14. Target Box

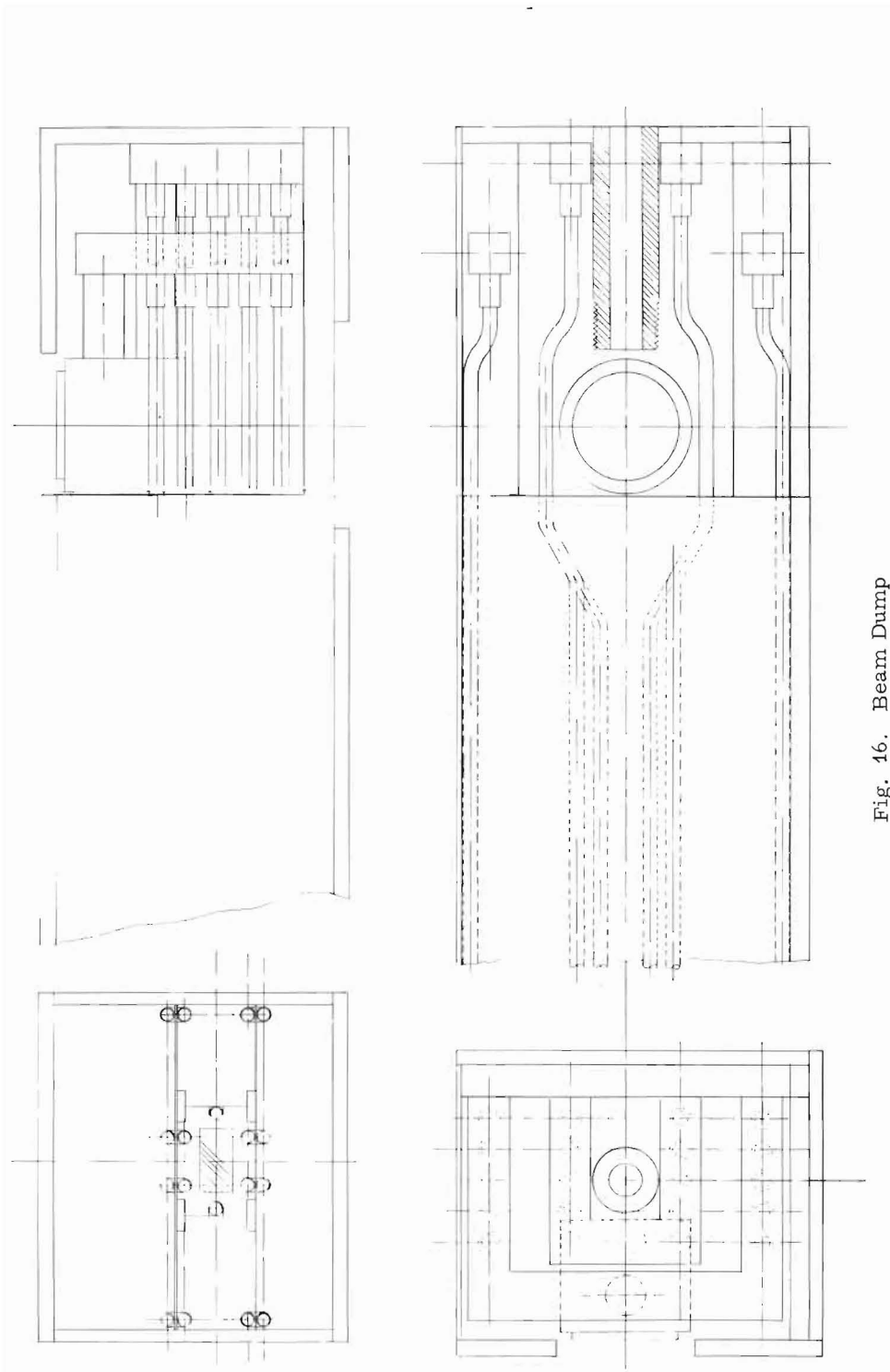


Fig. 16. Beam Dump

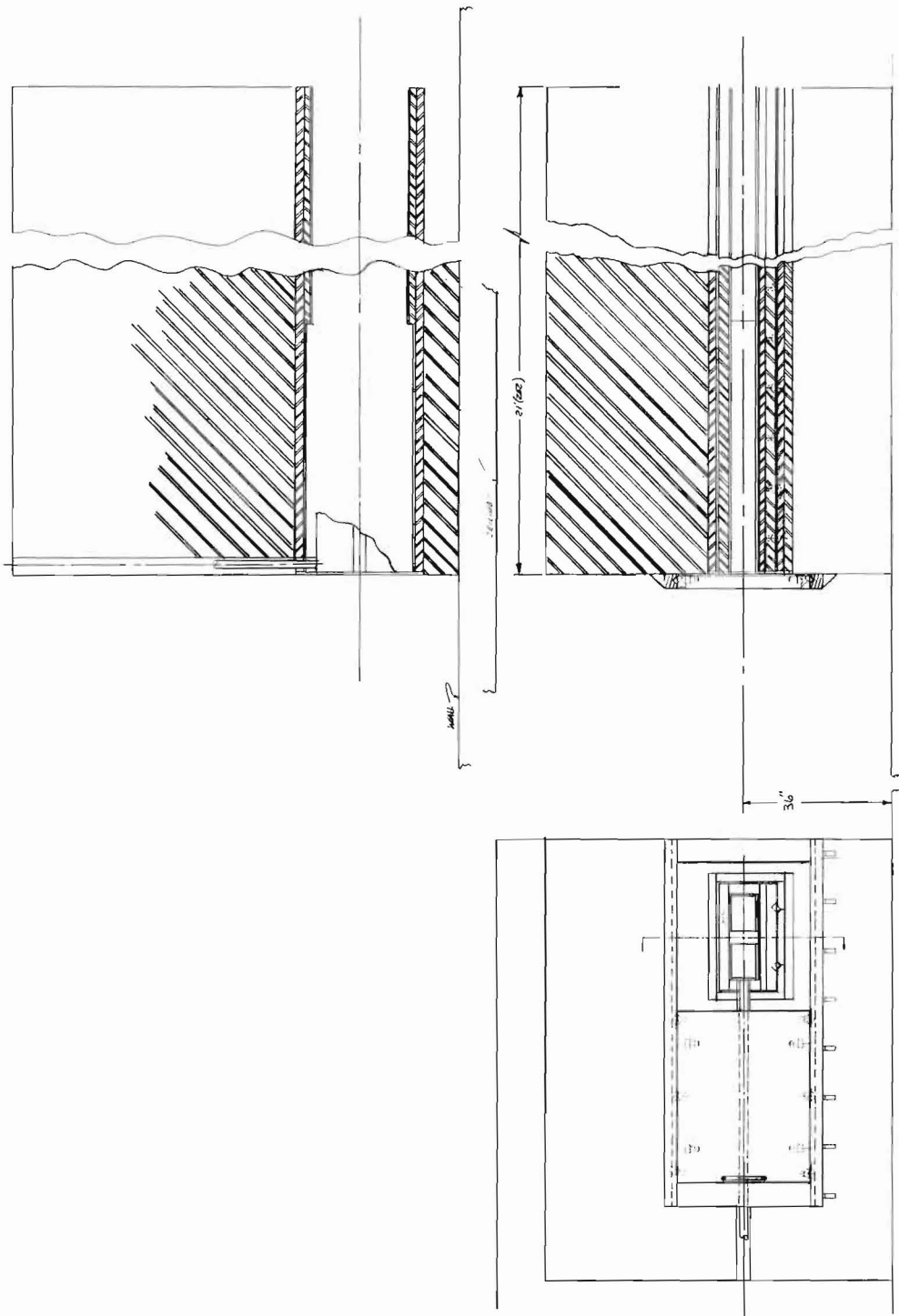


Fig. 17. Momentum Slit

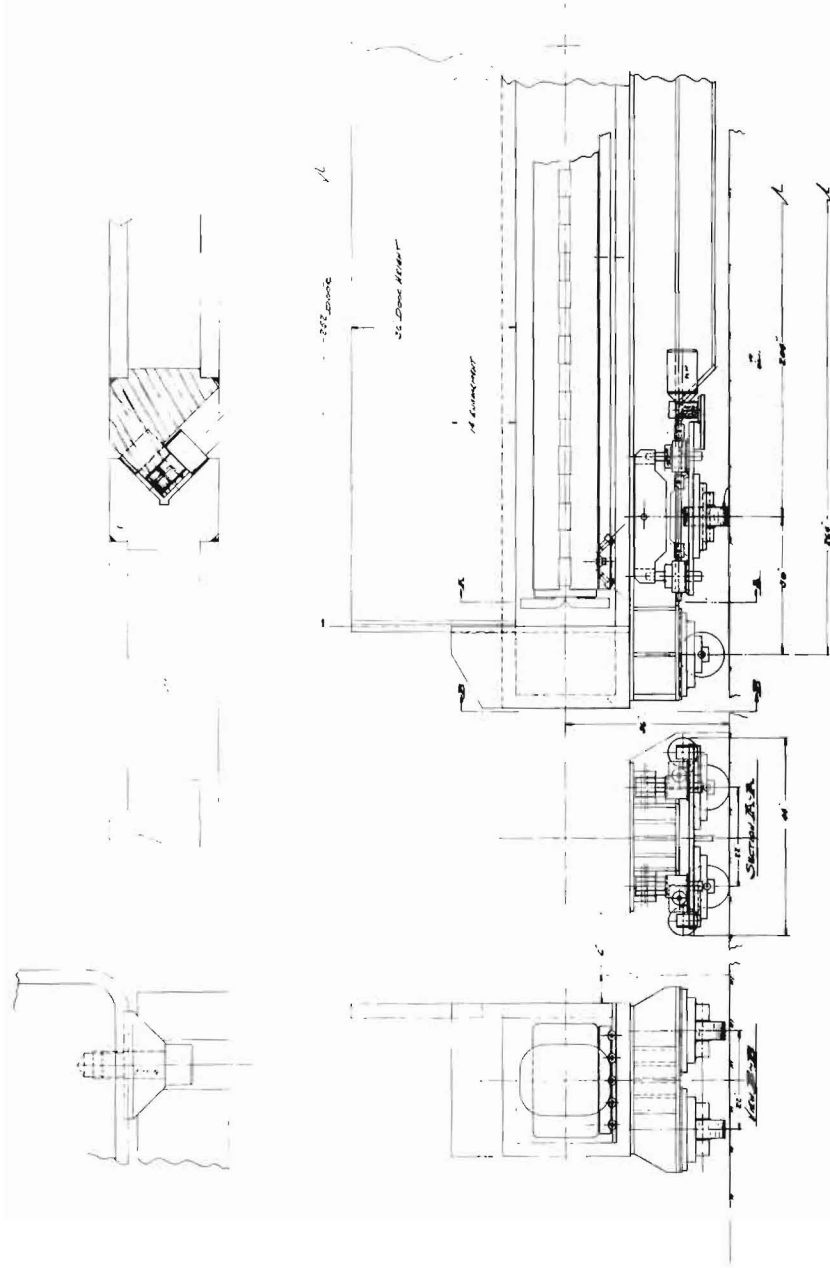


Fig. 18. Transporter

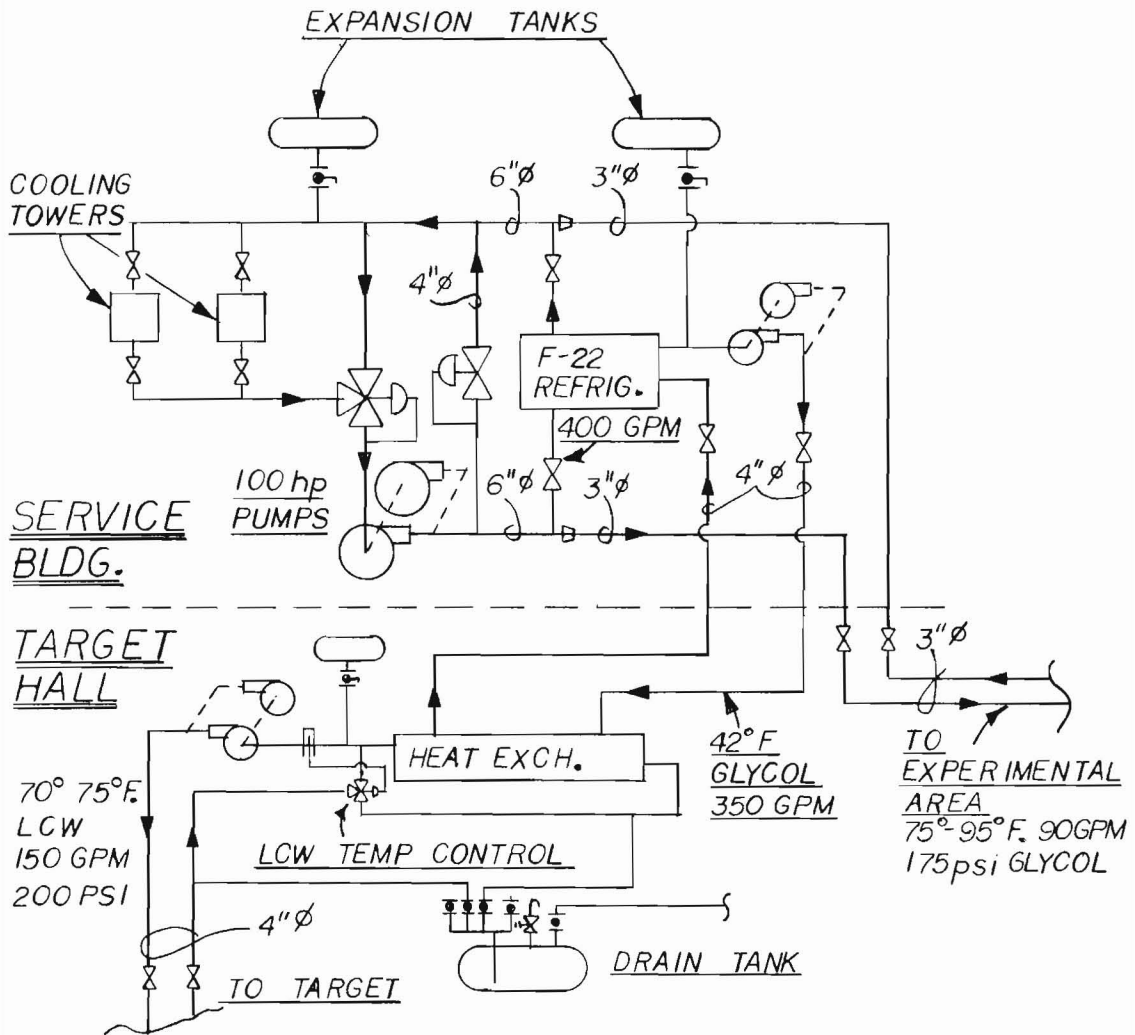


Fig. 19. Pion Lab Cooling Water System

